Title

Fabrication and characterization of bioprints with Lactobacillus crispatus for vaginal application.

Authors

Kyser, Anthony

Masigol, Mohammadali

Mahmoud, Mohamed

et al.

Publication Date

2023-05-01

DOI

10.1016/j.jconrel.2023.04.023

Peer reviewed

HHS Public Access

Author manuscript

J Control Release. Author manuscript; available in PMC 2024 May 01.

Published in final edited form as:

J Control Release. 2023 May ; 357: 545–560. doi:10.1016/j.jconrel.2023.04.023.

Fabrication and characterization of bioprints with *Lactobacillus crispatus* for vaginal application

Anthony J. Kyser[a,†], **Mohammadali Masigol**[b,†], **Mohamed Y. Mahmoud**[b,c], **Mark Ryan**[a], **Warren G. Lewis**[g,h], **Amanda L. Lewis**[g,h], **Hermann B. Frieboes**[a,b,d,e,*], **Jill M. Steinbach-Rankins**[a,b,d,f]

[a]Department of Bioengineering, University of Louisville Speed School of Engineering, Louisville, KY, 40202, USA

[b]Center for Predictive Medicine, University of Louisville, Louisville, KY, 40202, USA

[c]Department of Toxicology and Forensic Medicine, Faculty of Veterinary Medicine, Cairo University, Egypt

[d]Department of Pharmacology and Toxicology, University of Louisville School of Medicine, Louisville, KY, 40202, USA

[e]UofL Health – Brown Cancer Center, University of Louisville, KY, 40202, USA

[f]Department of Microbiology and Immunology, University of Louisville School of Medicine, Louisville, KY, USA

[g]Department of Obstetrics, Gynecology and Reproductive Sciences, University of California San Diego, La Jolla, California USA

[h]Glycobiology Research and Training Center, University of California San Diego, La Jolla, California USA

Abstract

Bacterial vaginosis (BV) is characterized by low levels of lactobacilli and overgrowth of potential pathogens in the female genital tract. Current antibiotic treatments often fail to treat BV in a sustained manner, and >50% of women experience recurrence within 6

[*]**Correspondence:** Hermann B. Frieboes, Department of Bioengineering, Lutz Hall 419, University of Louisville, KY 40208, USA. Tel.: 502-852-3302; Fax: 502-852-6806; hbfrie01@louisville.edu.

[†]Equal contribution

CRediT STATEMENT

Anthony J. Kyser: Data curation; Formal analysis; Investigation; Validation; Visualization; Roles/Writing - original draft; Writing - review & editing

Mohammadali Masigol: Data curation; Formal analysis; Investigation; Methodology; Validation; Visualization; Roles/Writing - original draft; Writing - review & editing

Mohamed Y. Mahmoud: Data curation; Formal analysis; Investigation; Validation; Visualization; Writing - review & editing

Mark Ryan: Data curation; Investigation

Warren G. Lewis: Formal analysis; Funding acquisition; Methodology, Writing - review & editing

Amanda L. Lewis: Formal analysis; Funding acquisition; Writing - review & editing

Hermann B. Frieboes: Formal analysis; Funding acquisition; Methodology; Project administration; Resources; Supervision; Writing - review & editing

Jill M. Steinbach-Rankins: Conceptualization; Formal analysis; Funding acquisition; Methodology; Project administration; Resources; Supervision; Writing - review & editing

months post-treatment. Recently, lactobacilli have shown promise for acting as probiotics by offering health benefits in BV. However, as with other active agents, probiotics often require intensive administration schedules incurring difficult user adherence. Three-dimensional (3D)-bioprinting enables fabrication of well-defined architectures with tunable release of active agents, including live mammalian cells, offering the potential for long-acting probiotic delivery. One promising bioink, gelatin alginate has been previously shown to provide structural stability, host compatibility, viable probiotic incorporation, and cellular nutrient diffusion. This study formulates and characterizes 3D-bioprinted *Lactobacillus crispatus*-containing gelatin alginate scaffolds for gynecologic applications. Different weight to volume (w/v) ratios of gelatin alginate were bioprinted to determine formulations with highest printing resolution, and different crosslinking reagents were evaluated for effect on scaffold integrity via mass loss and swelling measurements. Post-print viability, sustained-release, and vaginal keratinocyte cytotoxicity assays were conducted. A 10:2 (w/v) gelatin alginate formulation was selected based on line continuity and resolution, while degradation and swelling experiments demonstrated greatest structural stability with dual genipin and calcium crosslinking, showing minimal mass loss and swelling over 28 days. 3D-bioprinted *L. crispatus*-containing scaffolds demonstrated sustained release and proliferation of live bacteria over 28 days, without impacting viability of vaginal epithelial cells. This study provides *in vitro* evidence for 3D-bioprinted scaffolds as a novel strategy to sustain probiotic delivery with the ultimate goal of restoring vaginal lactobacilli following microbiological disturbances.

Keywords

Bacterial vaginosis; 3D bioprinting; probiotics; *Lactobacillus crispatus* ; female reproductive tract; women’s health

1. Introduction

Bacterial vaginosis (BV) is the most common vaginal condition in women of reproductive age[1, 2] with a global incidence of 23 to 29%[3]. BV is a condition characterized by diverse anaerobic and facultative bacteria such as *Gardnerella vaginalis (G. vaginalis)*[4–7] and *Prevotella bivia* within the vaginal microbiome. This stands in contrast to most individuals who have high levels of *Lactobacillus* in the vaginal niche. BV can result in symptoms including abnormal discharge and unpleasant odor. Serious adverse health outcomes have been associated with BV, including increased risk of sexually transmitted infections, postsurgical infection[8, 9], cervicitis and endometritis[10, 11], pelvic inflammatory disease, cervical cancer, and a variety of pregnancy complications[11–24].

Treatments for BV have only marginally progressed over the last fifty years[25]. Current treatments comprise administration of antibiotics alone, or, more recently, antibiotics with adjunct probiotic treatment[26]. While FDA-approved antibiotics, such as metronidazole, clindamycin, and tinidazole, are fairly effective in the initial resolution of BV symptoms[6, 27], recurrence rates of 50-70% within 12 months are an unfortunate reality[2]. These outcomes can be partly attributed to the action of some antibiotics on *Lactobacillus* species.

Furthermore, in recurrent BV, antibiotic treatment failure promotes bacterial antibiotic resistance. These factors contribute to BV recurrence rates as high as 66% [28, 29].

Due to the strong association of *Lactobacillus*-dominance with various positive health outcomes, a potentially promising approach to modulate the vaginal microbiome is to deliver probiotics, or living microorganisms that can provide health benefits to the host. A variety of lactobacilli are believed to exert beneficial activity by producing lactic acid and other antimicrobial compounds, and by competing with anaerobes in the vaginal environment. In particular, high levels of lactic acid reduce the vaginal pH, making the vaginal environment less hospitable to many microbes.

The benefits of daily probiotic treatments via oral or vaginal routes have been investigated in a variety of pathologies, including bacterial reproductive infections[6, 27, 30] and bacterial vaginosis[31–35]. Available dosage forms include topical creams, daily oral supplements, or daily to twice daily vaginal capsules, tablets, or suppositories[5, 25, 29, 36–39]. While oral treatments have been shown to deliver probiotics to the vagina, localized intravaginal delivery is often favored to increase bioavailability and colonization[25, 36, 40–45]. A variety of probiotic dosage forms have demonstrated clinical efficacy in BV[34, 38, 46–48]. For example, vaginal capsules and tablets, loaded with $10^8 – 10^9$ colony forming units (CFU) of either one or multiple *Lactobacillus* strains led to a potentially clinically relevant increase in clearance rate of BV after 6 months[49], while vaginal suppositories containing *Lactobacillus acidophilus* (*L. acidophilus)*, have been shown to provide localized and sustained probiotic delivery[50]. In addition, probiotics have been administered subsequent to antibiotic regimens to help restore the vaginal environment with beneficial bacteria after BV. One study administered oral clindamycin for seven days, followed by vaginal probiotic capsules for seven days [(10^9 *Lactobacillus casei rhamnosus* (LCR35)]. After one month, 83% of patients were reported as “cured” relative to 35% in the control group[51]. Recently, one of the most promising options has been shown in staging the delivery of probiotics with the antibiotic metronidazole, showing a decrease in BV recurrence and increased efficacy in eliminating BV, relative to antibiotic-only treatment[26].

Despite alleviating initial symptoms of BV, challenges exist with current probiotic (and antibiotic) dosage forms, which rely on frequent daily administration to obtain therapeutic effect. These dosing regimens may be difficult to achieve in practice for many women, leading to reduced efficacy. Additionally, barriers to convenience and ease-of-use, such as messiness, leakage, and unfavorable discharge, adversely affect user adherence and treatment efficacy[5, 7, 44, 52–55]. Relative to transient administration provided by tablets, suppositories, creams, and gels, one of the few platforms that has been designed to sustain probiotic[33, 56–60] (and other active agent[56, 61, 62]) delivery is the intravaginal ring (IVR). Pod-based IVRs containing lyophilized *Lactobacillus gasseri* (*L. gasseri)* and vaginal suppositories containing *L. acidophilus*, have been shown to provide localized and sustained probiotic delivery[50, 57]. An alternative for delivery of antibiotics or probiotics have been *in situ* gelling mucoadhesive hydrogels. Clotrimazole-loaded *in situ* gels demonstrated majority of drug release by 24 hr in developed formulations[63]. Hydrogels incorporating *Lactobacillus crispatus* (*L. crispatus*) displayed viscoelastic properties favorable for vaginal administration and inhibition of *Neisseria gonorrhoeae*[64]. Similarly conducted, *L. gasseri*-

loaded gelling formulations presented advantageous rheological strength suitable for vaginal application and preservation of probiotic[65].In another study, encapsulated calcium alginate beads of *L. gasseri* exhibited initial burst release of *L. gasseri* and shifts in pH[66]. Overall, although extended recovery of probiotic has been achieved with mucoadhesive hydrogel formulations, 3D-bioprinting may provide greater versatility in terms of geometrics and formulations for vaginal applications i.e., pH modulation, lower susceptibility to release changes, and favorable storage viability.

In contrast to the mold-based and often multi-step techniques typically involved in IVR fabrication, 3D-bioprinting enables the rapid manufacturing of scaffolds that can be tailored to individual patient conditions. Bioprinted scaffolds have historically been used to support or viably incorporate mammalian cells for a variety of biomedical applications. While bioprinted scaffolds have been more frequently developed as cell scaffolds, a variety of bioinks have incorporated different cell types in a high-throughput manner[67, 68]. In particular, bioinks composed of gelatin and alginate have been shown to promote high cell viability, scaffold stability, cellular nutrient diffusion, and co-delivery of multiple agents[69–72]. Gelatin-based hybrid materials are well characterized for localized delivery due to their physiochemical properties, biocompatibility, and, specifically for gelatin alginate, for biological activity that promotes live cell delivery [73]. Although alginate is not characterized as an antimicrobial, the material facilitates diffusion of antimicrobials to localized areas of infection to inhibit pathogenic growth[74]. The combination of gelatin and sodium alginate provides a hospitable environment for beneficial bacteria and supports the diffusion of antimicrobials produced by these bacteria. Recently, crosslinked gelatin alginate matrices loaded with chlorhexidine exhibited antibacterial activity against *Staphylococcus aureus* and *Escherichia coli* with evident areas of growth inhibition zones[75]. Additionally, Nisin-Z-loaded fibers blended from sodium alginate and gelatin fostered an antimicrobial effect upon *Staphylococcus aureus* as shown by its inhibiting effect on pathogen growth[76]. In parallel, technical advances have enabled the printing of diverse materials in spatially distinct layers to provide temporally modulated delivery regimens. Successes in attaining cell proliferation and differentiation for tissue engineering applications indicate significant potential for bacterial cells to retain viability, proliferate, and be released from bioprinted scaffolds.

Recent studies have incorporated prokaryotic cells during scaffold bioprinting[77–84]. 3D-bioprinting was utilized to develop gelatin alginate capsules containing probiotic bacteria for delivery to the small intestine, with the intention to improve the gut microbiome [85]. Additionally, gelatin alginate bioprints have been loaded with *Streptococcus zooepidemicus* for production of hyaluronic acid in biosynthesis applications such as wound healing [86]. Another study formulated a bioink containing genetically engineered *Escherichia coli* to secrete an anticancer drug, azurin, to remove toxins such as Bisphenol A and regulate bacterial growth [87]. Bioprinting gelatin alginate with bacteria also has been used to characterize pathogenic bacterial biofilms for antimicrobial resistance, for which three dimensional and thicker biofilms showed greater resistance [81]. These advancements support a trend towards using bioprinted bacteria as an alternative approach for physiological regeneration and *in vitro* pathogenic studies. The goal of this study was to fabricate and characterize novel 3D-bioprinted scaffolds that enable prolonged delivery and

proliferation of *L. crispatus* for eventual vaginal application. In comparison to other vaginal lactobacilli, *L. crispatus* offers greater colonization resistance, preventing overgrowth of other bacteria, and thus providing stability to the vaginal flora[88].Additionally, *L. crispatus* exhibits a higher magnitude of lactic acid production than other vaginal microbiome lactobacilli, e.g., enabling it to impede *Candida albicans* growth[89]. *L. crispatus* production of D(−)lactic acid contributes to superior antimicrobial potency to reduce infections as exemplified by inhibition of *Chlamydia trachomatis*[90]. Scaffold formulation, printability, degradation, and bacterial proliferation and release kinetics were evaluated. Ideal design criteria of 3D-bioprinted constructs included high line resolution with minimal line agglomeration, structural stability, high bacterial viability, and sustained probiotic release followed by proliferation for a minimum of one week. This work lays a foundation for future designs of delivery vehicles for sustained probiotic proliferation and release, with the ultimate goal of providing additional long-acting approaches for treating BV.

2. Materials and Methods

2.1 Materials

L. crispatus (MV-1A-US) was purchased from BEI Resources. Genipin and calcium chloride ($CaCl_2$) were obtained from Sigma Aldrich (St. Louis, MO). De Man, Rogosa, and Sharpe (MRS) broth (Sigma 69966) was used for culture of *L. crispatus* and scaffolds. The following were purchased to formulate simulated vaginal fluid: NaCl, KOH (Sigma, P-6310), $Ca(OH)_2$ (Sigma, 31219-100G), bovine serum albumin (Fisher, BP1600-100), lactic acid (Alfa Aesar, 36415), acetic acid (Fisher, A38-500), glycerol (VWR, M152-1L), urea (Alfa Aesar, A12360), and glucose (Sigma, G7021-1Kg) as described previously[91]. Phosphate buffer saline (PBS) was made with 137 mM NaCl (VWR, 0241-1kg), 2.7 mM KCl (Fisher, P217-500), 10 mM Na_2HPO_4 (Sigma, S9763-100G), and 1.8mM KH_2PO_4 (Sigma, P5655-100G).

2.2. Bacterial Culture

L. crispatus MV-1A-US was initially cultured on MRS (supplemented with 0.1% Tween 80) agar plates under anaerobic conditions at 37°C, and colony formation was observed after 48 hr. *L. crispatus* was then sub-cultured by selecting a single colony from the agar plates and culturing in 1 mL of MRS broth in a closed microcentrifuge tube at 37°C for an additional 24 hr in anaerobic conditions with 5% CO_2.

2.3 Bioink Preparation and Probiotic Incorporation

Bioinks were formulated from bovine skin gelatin (~MW=50 kDa) (Sigma, G9391-100G) and sodium alginate (~MW=26 kDa with β-D-mannuronic acid:α-L-guluronic acid (M:G) ratio of 1.56) (MP Biomedicals, 218295). Several different ratios of gelatin to alginate were tested, as most literature sources utilized 10 to 20% w/v gelatin and 1 to 5% w/v alginate to print mechanically stable constructs[72, 92–94]. MRS broth was used to dissolve the gelatin and sodium alginate in ratios of 10:1, 10:2, 11:2, 12:2, and 16:4 (w:w)/volume of MRS (hereafter w/v) (total polymeric concentrations of 15%, 16%, 17%, 18%, and 24% respectively), followed by overnight incubation at 37°C. Bioinks were then removed from the incubator, vortexed, and rested for 5 min before transferring to a syringe for subsequent

bioprinting. Blank scaffolds were bioprinted from bioink composed of gelatin:sodium alginate in MRS.

To fabricate *L. crispatus*-containing scaffolds, *L. crispatus* sub-cultures were diluted 1:10 in PBS. A Nanodrop 2000 (Thermo Scientific, MA) was utilized to measure the absorbance value (OD_{600}) to determine the volume of *L. crispatus* solution to add to the bioink, using the equation $y = ((9\cdot\times10^7)\cdot(x)) - 2\times10^7$ to obtain a theoretical loading of 5×10^7 CFU per mg scaffold. The appropriate volume of *L. crispatus* solution was centrifuged (3500×g, 10 min), supernatant was removed, and the pellet was resuspended in 500 μL of MRS. Bacteria were then added to 4.5 mL of prepared bioink, and then the bioink was thoroughly mixed and vortexed in biomedical safety cabinet. The bacteria-bioink mixture was transferred to a syringe for bioprinting. The CORE head of an Allevi 3 Bioprinter (Allevi, Inc., Philadelphia, PA) was heated to 37°C prior to bioprinting.

2.4 Bioprinting and Crosslinking of the Scaffolds

An Allevi 3 Bioprinter was used to bioprint blank and *L. crispatus*-containing scaffolds. The bioprinter was calibrated, and processing parameters including extruder temperature, pressure, and printing speed were optimized for printing. Extruder temperature was set at 37°C to decrease bioink viscosity and to simulate the physiological environment, while the initial extruding pressure was adjusted between 32 and 42 psi[95]. The temperature of the platform was neither heated nor cooled, and remained at room temperature during bioprinting. Gelatin to sodium alginate ratios of 10:1, 10:2, 11:2, 12:2, and 16:4 w/v were initially printed in layer thicknesses of 200 μm with a 30 G (152 μm inner diameter) needle to determine the printing formulation that provided the most accurate line resolution. Bioinks were loaded into 1 mL plastic syringes with a spatula, the syringe was placed in the extruder, and five different line formulations were printed to assess resolution and printing feasibility.

An extruded bioink formulation that displays consistent dimensions with the print files will validate and enable printing of more complex architectures. After determining the formulation that resulted in bioprints with accurate measurements of the desired construct, the needle gauge was varied to determine the effect on line resolution. Bioinks formulated in 10:2 w/v ratio were printed with 26, 30, or 34-gauge luer lock needle attached to the syringe. Pressures and extrusion rates were adjusted to adapt to changes in shear stress resulting from different needle diameters. Circle-shaped lattices were printed with diameters 30, 15, and 8 mm to determine resulting print resolutions with different needle gauges, with grid pattern set at 0.35 mm infill distance. Additionally, for each different lattice diameter/needle combination, scaffolds were printed with 1, 2, and 3 mm thicknesses. These circular lattice structures were printed with pre-made GCODE files that specified print dimension and geometry. Resulting prints were measured with a micrometer caliper. Printing parameters, determined from these experiments, were used to inform and fabricate subsequent intravaginal ring-type designs. The high-resolution circle-shaped lattice prints helped to inform the needle gauge needed to print a simpler, more appropriate intravaginal ring shape.

After determining the optimal parameters of formulation and needle gauge that best represented the input dimensions of diameter, line width and thickness, scaffolds were printed in intravaginal ring-shaped geometries to represent currently accepted dosage forms. IVR scaffolds were printed using a customized STereoLithography (STL) file specifying an outer diameter of 4 mm and inner diameter of 3 mm to correspond to murine vaginal sizes[96] for future *in vivo* studies. The optimized bioink used for printing contained 5×10^7 CFU/mg of *L. crispatus* at a 10:2 gelatin to sodium alginate ratio. The homogenous bioink was transferred to bioprinting syringe at a volume of 1 mL. Prior to printing, the CORE head of the Allevi 3 bioprinter was heated to 37°C to maintain an ideal physiological environment for *L. crispatus*. Extruder pressure was adjusted to 42 psi for a 30G needle to print constructs with accurate dimensions stated in the printing file.

Subsequent to printing, both blank and *L. crispatus* containing IVR-shaped scaffolds were placed in the refrigerator (4°C) for 15 min to harden. Two different crosslinkers, genipin and $CaCl_2$, were used to crosslink the gelatin and alginate portions of the scaffold, respectively. Genipin has been shown to improve gelatin mechanical and thermal properties of while maintaining drug permeation capabilities[97], as well as prolonging its degradation time[98], while $CaCl_2$ relies on ionic crosslinking to form a stable three-dimensional network providing mild reaction conditions, greater aqueous permeability, and increased stability of alginate after immersion in solute[99–101].

A variety of crosslinking conditions were evaluated to assess the effect of crosslinking molecule and time on scaffold integrity and probiotic viability: genipin-only (4 hr), genipin-only (24 hr), $CaCl_2$-only (20 min), $CaCl_2$ (20 min) and genipin (4 hr), and $CaCl_2$ (20 min) and genipin (24 hr). Uncrosslinked scaffolds were made for comparison to crosslinked groups. For dual-crosslinked scaffolds, $CaCl_2$ crosslinking was conducted prior to genipin crosslinking. Briefly, 20 mL of 10% w/v $CaCl_2$ in DI (deionized) water, using a Milli-DI® water purification system, were poured on the chilled scaffolds in a petri dish and scaffolds were chilled at 4°C for 20min. Next, 5 mL of 0.5% w/v[97, 102] genipin in 1×PBS was poured on the chilled scaffolds and incubated at room temperature for 4 or 24 hr[103]. Due to the temperature sensitivity of the crosslinking mechanisms, scaffolds were crosslinked by components separately, with calcium chloride crosslinking the alginate at lower temperature prior to the crosslinking of gelatin with genipin. Crosslinked scaffolds were then washed three times with DI water and placed back in the refrigerator until use. For $CaCl_2$-only or genipin-only crosslinked control groups, scaffolds were crosslinked and incubated for the durations and temperatures defined above.

2.5 Viscosity

Bioink viscosity was determined for the 10:2 w/v blank and *L. crispatus*-containing gelatin alginate formulations to ensure consistent bioink extrusion and resulting mechanically stable scaffolds. Similarly, 16:4 w/v bioinks served as a control group to compare difficult-to-print formulations. A DVE viscometer (AMETEK Brookfield, MA) was used to assess bioink viscosity and a rechargeable temperature data logger (Omega, CT) was used to measure the temperature with respect to time. Initially, 10 mL of the 10:2 gelatin alginate bioink was aliquoted to a scintillation vial and incubated at 37°C. The S63 spindle was submerged into

the bioink with spindle top 1 mm above surface, and temperature sensors were placed in the bioink to simultaneously record changes in viscosity and temperature. Viscometer was set to 20 rpm, and viscosity was measured as a function of temperature.

2.6 Degradation and Swelling

To assess mass loss, crosslinked scaffolds were dried at 50°C overnight to ensure scaffolds were fully dry, and the initial dry weight of the samples (W_i) was measured. Scaffolds were then immersed in 1.5 mL of simulated vaginal fluid (SVF) for 0, 4, 8, 24, 72, 120, and 168 hr, and 2, 3, and 4 weeks (wk), after which the final sample weight (W_f) was measured and re-immersed in fresh SVF. The 1.5 mL volume was chosen for representing a physiologically relevant cervicovaginal secretion volume previously observed in patients[104], Exposure to SVF provides physiologic pH and ionic functional salts for relevant interactions and represents a worst-case scenario for degradation. SVF best models the pH, osmolarity, and physiochemical interactions that would affect the durability and efficacy of intravaginal application [105]. As these scaffolds have mucoadhesive properties, swelling, biodegradability, and residence time are better determined in SVF [106, 107]. Mass loss percentage was determined according to Eq. (1):

$$\text{Mass Loss Percentage} = [(W_i - W_f)/W_i]\times 100 \quad (1)$$

To assess scaffold swelling, the initial mass of the crosslinked scaffolds (W_i) was measured. Scaffolds were placed in microcentrifuge tubes containing 1.5 mL SVF. Scaffold weights were evaluated at 0, 24, 48, 72, 96, 120, 144 and 168 hrs, and 2, 3, and 4 weeks (wk). At each time, scaffolds were removed, dried, and weighed to obtain the corresponding weight (W_s) and re-immersed in fresh SVF. Percent mass change relative to initial mass was determined according to Eq. (2):

$$\text{Mass Swelling Percentage} = [(W_s - W_i)/W_i]\times 100 \quad (2)$$

2.7 Bacterial Viability

After bioprinting, uncrosslinked blank and *L. crispatus*-containing scaffolds were assessed for viability after crosslinking for 0, 25, and 60 min at 4°C, conditions relevant to $CaCl_2$ crosslinking. The initial amount of bacteria inoculated into the complete bioink prior to printing was also enumerated. Pre-weighed, $CaCl_2$ crosslinked (non-genipin-crosslinked) samples were dissolved in 1 mL MRS broth at 37°C for 1 hr. The tubes were gently vortexed and 20 μL was serially diluted in 180 μL MRS broth. Aliquots of 5 μL were plated on MRS agar plates, placed in the anaerobic chamber for 48 hr, and the number of CFUs was counted.

2.8 Quantification of *L. crispatus* Release and Proliferation from Printed Scaffolds

Release and proliferation of *L. crispatus* was evaluated by placing crosslinked scaffolds in MRS broth for up to 4 wk with removal and washing of scaffolds at defined intervals. Pre-weighed scaffolds were placed in 1.5 mL microcentrifuge tubes and incubated in 1.5 mL MRS at 37°C with constant shaking at 150 rpm. MRS media provides a suitable *in vitro*

environment for proliferation due to nutrients similarly available in the vaginal microbiome. Supernatants from each sample were removed after 0, 4, 8, 24, 72, 120, 144, and 168 hr, and 2, 3, and 4 wk, then diluted by adding 20 μL to 180 μL of MRS broth. Five μL of each sample dilution were plated on MRS agar plates and placed in an anaerobic chamber for 48 hr. After 48 hr, plates the CFU were enumerated. After each collection, scaffolds were washed four times in 5 mL PBS, placed in 1.5 mL fresh MRS broth, and incubated until the next time point.

2.9 Quantification of Lactic Acid and pH

Scaffolds were incubated in MRS media and the materials in suspension were collected at the corresponding time points (0, 24, 48, 72, 96, 120, 144, and 168 hr, and 2, 3, and 4 wk) were evaluated for lactic acid levels and pH. Briefly, 1 mL of suspension was centrifuged at 2500×g for 5 min to separate any bacteria from the media supernatant. The solution was then subjected to 10-fold serial dilutions. Concentrations of L- and D-lactic acid were determined with a D-Lactic acid/L-lactic acid detection kit (R-biopharma; Darmstadt, Germany) and the corresponding pH of supernatants at each time point was estimated using pH strips (Fisher Scientific) with a pH range of 1 to 6 and an accuracy of 0.5 pH units.

2.10 Probiotic Stability in Bioprinted Scaffolds after Storage

Temperature stability of *L. crispatus* formulated in 10:2 gelatin:alginate bioprinted scaffolds was tested by CFU counting on MRS agar, as described above. Scaffolds containing *L. crispatus* were stored in sealed Petri dishes at −20°C, 4°C, or 20°C, and probiotic viability evaluated for up to 4 wk. After 1, 2, and 4 wk, the stored scaffolds were placed in microcentrifuge tubes and incubated in fresh 1.5 mL MRS broth at 37°C with constant shaking at 150 rpm, and daily release and resulting proliferation in MRS were assessed from the scaffold at 0, 24, 48, 72, 96, 120, 144, and 168 hr. Scaffolds were washed four times in 5 mL PBS, placed in 1.5 mL fresh MRS broth, and incubated until the next time point. Release was diluted using 10-fold serial dilutions, 5 μL was plated on MRS agar plates, and CFUs were counted after 48 hr of anaerobic incubation at 37°C. Cumulative release and proliferation of *L. crispatus* in MRS from scaffolds were evaluated for and compared to scaffolds assessed immediately post-fabrication.

2.11 Scaffold Morphology

Morphology of the blank and *L. crispatus*-containing scaffolds was characterized using scanning electron microscopy (SEM). Scaffold cross-sections were placed on carbon tape, sputter-coated with a layer of palladium/gold alloy (8.5 nm) and imaged using Apreo C LoVac Field Emission SEM (Thermo Scientific, Waltham, MA). Proliferation was compared in scaffolds that were immersed in timepoints at 0, 1, and 7 d in MRS and SVF.

2.12. VK2/E6E7 Viability

An MTT assay was used to determine preliminary *in vitro* safety of $CaCl_2$ and genipin crosslinked, blank and *L. crispatus*-containing scaffolds, with a VK2/E6E7 cell line. Cells were plated at a density of 300,000/well in 12-well plates and incubated for 24 hr at 37°C. Media only (untreated cells) and 10% DMSO were used as viable and non-viable cell

controls. After 24 and 72 hr incubation, 100 μL of MTT labeling reagent was added to each well and incubated at 37°C for 4 hr, followed by adding 100 μL of lysis buffer containing 10% sodium dodecyl sulfate and 0.01 M hydrochloric acid. After 16 hr incubation, the absorbance was read at 570 nm (SYNERGY Microplate Reader, Biotek Instruments Inc) and normalized to cell-only absorbance to attain the relative percent of cell viability.

2.13. Lactic Dehydrogenase (LDH) Assay

Loss of membrane integrity and resulting leakage of cellular contents was estimated by measuring the release of cytosolic enzyme LDH. Extracellular LDH activity was quantified using CytoTox96® non-radioactive cytotoxicity assay (Promega, Madison WI) as described by the manufacturer. VK2/E6E7 cells were plated at density of 300,000 cells in 1 mL media per well in a 12-well flat bottom plate, and incubated at 37°C, 5% CO_2 for 24 hr. $CaCl_2$ and genipin crosslinked, blank and *L. crispatus*-containing scaffolds were added to cells in triplicate for 24 h and 72 hr at 37°C in 5% CO_2. Fifty μL of supernatant from treated cells were added to the LDH substrate and incubated at room temperature for 30 min. Reactions were subsequently terminated by adding 50 μL of the provided stop solution. LDH activity was determined by measuring optical density at 490 nm. Cells treated with 1 ng of staurosporine, used to cause cell death, or medium-only served as positive and negative controls, respectively. Cellular leakage of LDH was calculated as percentage absorbance of each sample relative to negative controls.

2.14. Inhibition of *G. vaginalis* Growth

This experiment was performed to evaluate the effect of *L. crispatus*-loaded bioprinted scaffolds on *G. vaginalis* growth in the presence of VK2/E6E7 vaginal epithelial cells. In a 48-well plate, 250 μL of 1 day (9×10^7 CFU/mL), 3 day (2×10^8 CFU/mL), and 7 day (4×10^8 CFU/mL) scaffold culture supernatant were added to each of three wells containing ~90% confluent VK2/E6E7 cells in 250 μL of antibiotic-free cell media. The 48-well plate was then incubated in 5% CO_2 at 37°C for 1 hour to protect VK2 cells against *G. vaginalis*. After incubation, 250 μL of 1×10^6 CFU/mL *G. vaginalis* were added to each well and incubated in 5% CO_2 at 37°C for 24 hr. After 24 hr incubation, VK2 cells were washed twice with 1× Sterile PBS post removal of supernatant. Afterward, cells were lysed by incubation with one mL of sterile water for 30 min at 37˚C in 5% CO_2. Cell suspensions were serially diluted and 5 μL of each dilution were plated on NYC III (with 1 mg/mL streptomycin sulfate salt) and MRS agar plates, and incubated anaerobically at 37°C. Colony forming units were counted after 48 hr. Controls included free *L. crispatus* (5×10^7 CFU/mL) alone, *L. crispatus* in culture with *G. vaginalis* (1×10^6 CFU/mL), and free *G. vaginalis* (1×10^6 CFU/mL) alone. A blank scaffold, containing no bacteria, was fabricated and its supernatant used as a negative control.

2.15 Statistical Analysis

All experiments were done in triplicate, and Minitab (Minitab, LLC, State College, PA) and GraphPad (GraphPad Software, La Jolla, CA) were used for statistical analysis. Three replicates were used for each sample and subjected to Grubbs' test ($p \leq 0.05$) to determine outliers to be removed. All statistical analyses in GraphPad Prism (version 9.3.1) were performed using one-way ANOVA with Tukey multiple comparison's test ($p \leq 0.05$).

3. Results

3.1 Bioprinting of Probiotic-Containing Scaffolds

The printing resolution affects the scaffold shape and structure. In order to achieve sustained probiotic delivery, bioink formulation and printing parameters were determined by evaluating printing resolution to ensure scaffolds retained shape and structure conducive to controlled and sustained release. Accordingly, the bioink formulation ratio was varied to assess its impact on line resolution and scaffold integrity with a standard-gauge needle after printing.

First, line resolutions of blank and *L. crispatus*-containing gelatin:alginate (10:1, 10:2, 11:2, 12:2, 16:4 (w:w)/v (hereafter w/v) formulations based on previous studies[72, 92–94] were evaluated as potential candidates (Figure 1). These formulations were chosen with the goal to maintain structure when printed. An image of the bioprinted lines resulting from initial prints are shown in Figure 1, respectively. Overall, 10:2 and 12:2 w/v blank formulations, composed of solely gelatin:sodium alginate and MRS, were found to provide the most line continuity and closest line resolution relative to input dimensions, whereas 10:1 and 11:2 formulations resulted in thicker and thinner lines, respectively. In comparison, the 16:4 formulation resulted in line fragmentation, with an overall asymmetrical and jagged appearance.

Upon addition of *L. crispatus*, 10:1, 11:2, and 12:2 w/v formulations resulted in line broadening, in addition to line fragmentation and inconsistent extrusions, while the 16:4 w/v formulation displaying asymmetrical and jagged morphology. Overall, 10:1, 11:2, and 12:2 w/v prints showed a 2-fold increase in width when *L. crispatus* was incorporated (spanning ~0.90-1.65 mm, with respect to the input line width of 0.68 mm), contributing to a decrease in line resolution. In contrast, the 10:2 w/v blank and *L. crispatus*-containing bioinks exhibited the finest line resolution and ability to maintain structural integrity, with line widths of 0.76±0.06 mm and 0.78±0.03 mm, respectively. Therefore, the 10:2 formulation was selected for subsequent studies.

Next, the effects of needle gauge and *L. crispatus* addition were evaluated for the 10:2 formulation. A variety of circle-shaped lattice structures were printed with varying diameters and thicknesses, with 26G, 30G, and 34G needles selected for fine-tuned gelatin alginate printing (Figure 2). Blank and *L. crispatus*-containing bioprints are shown in **top** and **bottom row**, respectively. Scaffold diameter and thickness were varied between 8, 15, and 30 mm and 1, 2, and 3 mm (here, for each 3×3 panel) to adequately assess the range of printing resolution in distance and layer thickness.

Overall, uniform bioink extrusion was achieved with pressures of 42 and 115 psi, and 30G and 34G needles, respectively. Well-defined structures were unachievable with the larger 26G needle, regardless of pressure, for blank or *L. crispatus*-containing scaffolds. For most bioprints, the 34G needle maintained infill spaces and resolution of both blank and *L. crispatus*-containing lattice structures, whereas 26G and 30G needles resulted in amorphous *L-crispatus*-containing lattice structures. Based on these observations, the 34G needle was chosen to print subsequent scaffolds.

In parallel, printing integrity was evaluated as a function of *L. crispatus* loading (10^7, 10^8, and 10^9 CFU per mg scaffold) as a function of scaffold thickness and diameter (Figure 2B and Figure 2C). Thicknesses and diameters of resulting scaffolds were measured as a function of probiotic concentration at 4 different positions within the circle-shaped structures. Generally, as probiotic concentration increased, scaffold thickness and diameter increased (Figure 2B and Figure 2C). As one example, 8 mm diameter scaffolds printed with thicknesses of 2mm, showed an initial thickness of 1.82 mm for blank scaffolds, subsequently increasing to 1.92, 2.05, and 2.31 mm for 10^7, 10^8, and 10^9 CFU *L. crispatus* per mg scaffold. Additionally, as the input scaffold thickness increased from 1 to 3 mm, the deviation in thicknesses increased for blank and *L. crispatus*-containing formulations.

Somewhat similar trends were observed for 1 mm thick scaffolds printed with a 15 mm diameter (Figure 2C). Average printed diameter of 15 mm scaffolds increased from 14.97 mm, for blank scaffolds to 14.52, 16.18, and 18.38 mm for scaffolds containing 10^7, 10^8, and 10^9 CFU *L. crispatus* per mg scaffold. Scaffolds printed in 8 and 30 mm diameters showed minimal changes in diameter as a function of probiotic incorporation, with statistical significance observed only for the 8 and 15 mm diameter scaffolds (blank to 10^9 CFU/mg). Overall, scaffolds containing 10^7 CFU/mg provided the closest lattice print dimensions to blank scaffolds, in both thickness and diameter. Moreover, the loading of *L. crispatus* concentration was more significant when considering thickness of scaffolds, leading to less reproducibility and maintenance of line resolution at increased scaffold thicknesses and bacterial concentration. To maximize loading, while still achieving printing accuracy, subsequent scaffolds were printed with a theoretical loading of 5×10^7 CFU *L. crispatus*/mg.

3.2 Ink Viscosity

Bioink viscosity was evaluated as a function of temperature for the 10:2 and 16:4 w/v (control) blank and *L. crispatus*-containing formulations, due to the temperature dependence of probiotic viability. Results were also obtained for the sub-optimal 16:4 w/v formulation to quantify the associated discrepancy in viscous behavior and how it might correspond to the ink resolution. At 37°C, the viscosities of 10:2 w/v blank and *L. crispatus*-containing (5×10^7 CFU/mg) gelatin alginate bioinks were 1171±17 mPa·s and 1616±19 mPa·s, respectively. As temperature decreased from 37°C to 28°C, both blank and *L. crispatus*-containing 10:2 formulations showed steady increases in viscosity, resulting in viscosities of 1989±23 mPa·s and 2501±19 mPa·s, respectively (Supplementary Figure 1A). Similar trends were observed with the 16:4 w/v formulation, however initial viscosities (at 37°C) of blank and *L. crispatus*-containing (5×10^7 CFU/mg) bioinks were much higher with values of 155±13 and 125±1 Pa·s (Supplementary Figure 1B). As temperature decreased from 37°C to 30°C, blank and *L. crispatus*-containing 16:4 formulations showed an initially steady increase in viscosity. Below 30°C the *L. crispatus*-containing bioink had a sharp increase in viscosity; at 28°C, blank and *L. crispatus*-containing bioinks had viscosities of 270±28 Pa·s and 507±55 Pa·s, respectively.

3.3 Scaffold Degradation and Swelling as a Function of Crosslinking Conditions

Crosslinking conditions and durations were varied to evaluate mass loss and degradation for ring geometries printed with the selected 10:2 w/v gelatin alginate formulation and

loaded with 5×10^7 CFU *L. crispatus*/mg. Degradation and swelling of scaffolds in SVF provided the best simulation *in vitro* of physiological physiochemical interactions in the vagina,. Macrostructural observations showed that dual-crosslinking with $CaCl_2$ followed by genipin was most resistant to degradation over 28 d (Figure 3A), while crosslinking solely with genipin (Figure 3B) or $CaCl_2$ (data not shown) resulted in degradation within 7 or 1 d, respectively. Furthermore, scaffolds crosslinked with genipin-only were fully degraded within 7 d, independent of 4 or 24 hr crosslinking duration. Similarly, dual-crosslinking with both $CaCl_2$ and genipin for only 4 hr resulted in rapidly degraded structures, on the order of 7 d, while dual-crosslinking for 24 hr resulted in intact structures over 28 d (Figure 3A).

Scaffold degradation was quantified by measuring mass loss of oven-dried scaffolds with respect to time (Figure 3B). Average mass of dual-crosslinked scaffold printed with 5×10^7 CFU *L. crispatus*/mg was 2.21±0.25 mg. Overall, initial mass loss occurred within first 4 to 8 d and stabilized after these durations. After 24 hr, dual-crosslinked and genipin-only crosslinked scaffolds (crosslinked for 24 hr) lost 16 and 19% of their initial mass, respectively. After 28 d, small differences in mass loss were observed between dual- and genipin-only crosslinked scaffolds ($p\leq0.0001$), with total mass losses of 25% and 38% of initial mass, respectively.

Scaffold swelling was quantified by measuring the mass of tissue-blotted scaffolds relative to their initial mass (Figure 3C). After 24 hr, dual-crosslinked scaffolds exhibited 18±6% mass loss, relative to the 24±5% mass loss observed after crosslinking with genipin-only. After 28 d, both dual- and genipin-only crosslinked scaffolds showed mass loss up to 45% of initial value. Overall, minimal differences in scaffold swelling, as measured by mass change, were observed between dual- and single-crosslinked groups.

3.4 *L. crispatus* Viability in Scaffolds

Bioprinted scaffolds containing 1×10^7, 5×10^7, and 1×10^8 CFU *L. crispatus* (based on optical density) per mg scaffold, covered a range of acceptable resolutions compared to blank (Figure 2B–C). Bacteria were grown from the printed scaffolds after $CaCl_2$ crosslinking for 0, 25, and 60 min at 4°C (Figure 4A). The *L. crispatus* within scaffolds maintained viability after up to 60 min of calcium crosslinking. Visual inspection made evident that the architecture of blank and *L. crispatus*-containing scaffolds remained intact after immersion in SVF for 28 d (Figure 4B).

Next, the extent to which scaffolds were capable of continued recovery of *L. crispatus* was investigated. Release and proliferation of *L. crispatus* from scaffolds into nutritive media (MRS), as best representation and detection of *L. crispatus* capabilities of proliferation, pH modulation, and antimicrobial production *in vitro*, were evaluated over 4 wk (Figures 4C). After 24 hr and 14 d, cumulative probiotic recovery from the scaffolds reached 10^8 and 5×10^9 CFU/mg, while after 28 d, concentrations reached 10^{10} CFU/mg (Figure 4D). Daily recovery showed relatively steady concentrations of approximately 4×10^8 CFU/mg released per day (Supplementary Figure 2).

To evaluate the metabolic activity of *L. crispatus*-containing dual- and genipin-only crosslinked scaffolds, D- and L-lactic acid were measured following the proliferation of

L. crispatus (Figure 4E). Lactic acid and pH modulation were evaluated in MRS to highlight the *L. crispatus* antimicrobial production and ability to modulate an environment at higher pH. Levels of lactic acid were concordant with the observed release and proliferation of bacteria from the scaffolds. Genipin-only and dual-crosslinked *L. crispatus*-containing scaffolds resulted in total measurements of 38.8 and 40.7 mg of D-lactic acid/mg scaffold and produced 18.5 and 19.1 mg of L-lactic acid/mg scaffold, respectively, over 4 wk in MRS.

Lastly, the ability of *L. crispatus* recovered from dual- and genipin-only crosslinked scaffolds to modulate the surrounding pH was measured in media supernatant after daily media changes (Figure 4F). In congruence with lactate levels, the pH of serially removed supernatants decreased from 6 to 3.5 after ~4 d of dual-crosslinked scaffold immersion in MRS. Genipin-only scaffolds showed a slightly more gradual decrease in pH, achieving comparable pH levels (3.5) after 5 d. Both genipin and dual-crosslinked scaffolds demonstrated lowered pH values after ~4 or 5 d, indicative of bacterial viability and metabolic activity.

3.5 Stability of *L. crispatus* in Scaffolds

Stability of *L. crispatus* was assessed by measuring recovery from scaffolds after storage at −20°C, 4°C, and 20°C for 4 wk (Figure 5). After storage at −20°C for multiple weeks (Figure 5A), scaffolds demonstrated viable probiotic recovery for up to 7 d, similar to freshly made unstored scaffolds. After storage at 4°C, samples stored for 1, 2 and 4 wk showed a slight reduction in viability over 7 d, relative to fresh scaffolds, but similar viability with respect to each other (Figure 5B). In comparison, samples stored at room temperature (Figure 5C) lost viability.

3.6 Scaffold Characterization

SEM images of blank and *L. crispatus*-containing scaffolds, dual-crosslinked with $CaCl_2$ (20 min) followed by genipin (24hr), are shown in (Supplementary Figure 3). Proliferation, relative to that in blank scaffolds, was visually evident from cross-sectional images between 1 and 7 d. Presence of *L. crispatus* in the interior cross-section demonstrates the potential of *L. crispatus* to proliferate in the bioprinted scaffolds.

3.7. VK2/E6E7 Viability

Viability of vaginal keratinocytes (VK2/E6E7) was evaluated after treatment with blank and *L. crispatus*-containing scaffolds, crosslinked with different crosslinkers (Figure 6A). Vaginal keratinocyte viability was maintained after 24 and 72 hr treatment with all scaffold groups, relative to untreated VK/E6E7 cells. Blank genipin-only and dual-crosslinked *L. crispatus*-containing scaffolds maintained greater than 96% cell viability over 24 and 72hr treatment conditions. Uncrosslinked and $CaCl_2$-only crosslinked blank scaffolds showed a slight increase in viability after 24 and 72hr, relative to untreated cells. In contrast, cell viability for negative control group, 10% DMSO, had viability of 28 and 33%, respectively, of that observed with untreated cells.

3.8. Lactic Dehydrogenase (LDH) Release Assay

LDH release was measured as a marker for cell membrane integrity after treatment with blank and *L. crispatus*-containing scaffolds, crosslinked with different crosslinkers. Figure 6B shows that LDH levels released from vaginal keratinocytes (VK2/E6E7 cells) treated with all scaffolds were negligible relative to control untreated cells. It was confirmed that there was no significant difference in LDH levels between untreated cells and cells treated with *L. crispatus*. However, LDH released from cells treated with staurosporine was significantly higher ($p \leq 0.0001$) than control or treated cells, indicating that the scaffolds did not compromise cell membrane integrity.

3.9. *L. crispatus* -containing Bioprinted Scaffolds Inhibit *G. vaginalis* Growth

G. vaginalis viability was evaluated when co-cultured with *L. crispatus* supernatants recovered from bioprinted scaffolds at different time points in the presence of VK2 cells for 24 hr (Figure 7). One-day supernatant, 7.79 log CFU/mL of *L. crispatus*, significantly ($p \leq 0.0001$) inhibited the viability of *G. vaginalis* by 4.32-log relative to free *G. vaginalis*. Also, supernatant of three-day incubation, 8.67-log CFU/mL of *L. crispatus*, significantly ($p \leq 0.0001$) inhibited *G. vaginalis* growth by 4.98-log relative to free *G. vaginalis*. Seven-day supernatant, 8.73-log CFU/mL of *L. crispatus*. demonstrated the highest inhibition by 5.36-log relative to free *G. vaginalis*. This inhibition was significantly ($p \leq 0.05$) higher than that of the one-day supernatant. Lastly, free *L. crispatus*, 5×10^7 CFU/mL, significantly ($p \leq 0.0001$) inhibited *G. vaginalis* growth by 4.74-log compared to free *G. vaginalis.*

4. Discussion

The administration of probiotics has shown promise as an alternative or adjunct to antibiotics to treat BV[5, 34, 38, 46–48]. Probiotics can improve well-being by producing antimicrobials and acidic pH, among other possible mechanisms[5, 108, 109]. One of the primary challenges in both oral and intravaginal delivery is user adherence. In particular, the frequent, once-to-twice daily administration needed for antibiotic and probiotic therapy is difficult to achieve in practice. One potential solution is to develop sustained release dosage forms that enable prolonged active agent delivery, such as probiotics, over a duration of days to weeks. To date, vaginal tablets, gels/creams, films, capsules, microparticles, intravaginal rings (IVRs), and suppositories have been locally delivered to the female reproductive tract. To our knowledge, pod-based IVRs containing lyophilized *L. gasseri*, have been the only platform shown to provide sustained probiotic delivery *in vitro*[33, 110].

Recently, 3D-bioprinting has emerged from additive manufacturing as a new alternative to fabricate materials for broad applications, including tissue and organ regeneration, biological implants, and drug and biologic delivery[68, 77, 78, 81, 82, 111, 112]. Specifically bioprinting can incorporate and deliver live cells from a variety of materials. In 3D-bioprinting, cell-containing bioinks can be extruded at temperatures and pressures compatible with physiological conditions, while maintaining cell viability, in an aseptic/sterile environment[113–115]. Due to its success in incorporating both eukaryotic and prokaryotic cells[69–72, 79, 116, 117], this study sought to apply bioprinting to develop novel scaffolds that could prolong probiotic release and proliferation targeting the vaginal

environment for durations of days to weeks. A variety of bioinks have been used for biological printing, some of which include collagen, gelatin, fibronectin, laminin, chitosan, alginate, and silk fibroin[118]. For this work, gelatin alginate was selected due to successes in bioprinting eukaryotic cells for grafting and regenerative medicine applications[69–72], and, more recently, to deliver viable prokaryotic cells while maintaining scaffold integrity[79, 116, 117]. More broadly, bioprinting has the potential to create precisely designed scaffolds that adopt a streamlined additive manufacturing process, enable the incorporation of biologics, and are relatively inexpensive and rapid to fabricate, relative to custom molding processes[78, 79, 83]. Furthermore, bioprinting enables customized architectures to match user preference and to tune release of active agents in personally tailored products. Hydrogels have been used in localized intravaginal delivery to treat vaginal bacterial infections and BV [119, 120]; however, duration of controlled release of active agents from hydrogels is on a shorter timeframe than gelatin alginate 3D printed scaffolds, limiting their ability to promote lactobacilli that could help repopulate and re-establish the vaginal flora. The expansion of bioprinting to female genital tract applications and, more specifically, to treat conditions related to the microbiome and infection, may offer a novel and alternative methods to address longstanding problems in women's health.

This study began by assessing the reproducibility of bioprinting different gelatin alginate formulations with and without the incorporation of probiotics. Bioink homogeneity is an important parameter, first to attain uniform printability and second, to enable nutrient diffusion and hence *L. crispatus* viability in the bioink during and post-printing. A variety of gelatin alginate formulations were evaluated to determine the changes in line printing resolution and morphology when *L. crispatus* was incorporated into the bioink[72, 92–94]. Of the tested formulations, the 10:2 *L. crispatus*-containing gelatin alginate bioink provided the most accurate line resolution with respect to the specified input line dimensions, with a difference in line width of only 2.5% between the blank and *L. crispatus*-containing 10:2 formulation (Figure 1).

In addition to the fundamentals of maintaining line resolution, bioprinting also relies upon parameters such as infill density, extrusion flow rate and pressure, needle gauge, and layer thickness – all contingent on the selected bioink formulation. To investigate the impact of some of these parameters, blank and probiotic-containing lattice structures were bioprinted with a variety of thicknesses and diameters (Figure 2A). From these lattice structures, the 34G needle printed with the greatest precision, evident from the achieved infill densities. Overall, it was observed that as the lattice thickness increased, the variation in scaffold thickness from the input value increased (Figure 2B), while less variation was seen with changes in the diameter. These results suggest that the weight and viscosity of the bioink may play a more important role in achieving a non-disperse or high-resolution structure. It has been observed that incorporating different variations of cell density in gelatin bioink can yield variations in viscosity and impaired printing resolution [121], a phenomenon similarly observed with this study's printing resolution when loading different *L. crispatus* concentrations (Figure 2). Consequently, 1 mm scaffold thickness was selected, building upon previous knowledge of how bioprinting gelatin alginate thicknesses influence biofilm formation, for which greater formation was evident in thinner constructs [81]. Scaffold thickness and diameter increased at high probiotic loading (blank vs. 10^9 CFU/mg, 1 and

2 mm) and (blank vs. 10^9 CFU/mg, 8 and 15 mm), respectively (Figure 2). As expected, as scaffold thickness increases, more variation in structure may be expected, in particular, for more viscous bioinks as seen with *L. crispatus*-containing bioinks. The 10^7 CFU/mg *L. crispatus*-containing bioink was found to provide prints most closely aligned with the thickness input dimensions. Similar to the findings of other studies, these results indicate that the architecture should strive to achieve accurate printing outputs, as prior work has shown that size deviations may induce more rapid release of active agents[62, 122] and compromise mechanical integrity. In contrast to molding techniques, extrusion 3D-printed constructs can be built with accurate dimensions (via computer-aided design; CAD) with uniform active pharmaceutical ingredient (API) incorporation, whereas molds may deviate from desired dimensions and possess structural irregularities, as well as less accurate personalized dosing adjustments [123]. More pertinent to vaginal applications, molds have been shown to have faster API release compared to extruded prints [124], making them a less attractive option for sustained delivery applications.

In parallel with measuring the line resolution of bioprinted lattice structures, bioink viscosity was evaluated to determine the role of the *L. crispatus* inclusion on printing resolution. Studies with gelatin alginate have found printability within similar viscosity ranges (~1000 mPa·s) [125–127] to the 10:2 blank and *L. crispatus*-containing formulations in this study, with viscosities of 1171±17 mPa·s and 1616±19mPa·s at 37°C, respectively (Supplementary Figure 1A). Overall, the 10:2 and the more viscous, 16:4 formulations showed similar trends of increasing viscosity as a function of decreasing temperature; however, the 16:4 formulation exhibited >100-fold increase in viscosity at 28°C compared to the other formulation. It has been observed that gelatin bioink with variations of cell density yielded corresponding variations in viscosity and potentially impaired printing resolution [121],a phenomenon similarly observed with this study's printing resolution when loading different *L. crispatus* concentrations (Figure 2). Differences in viscosity between the 10:2 and 16:4 gelatin alginate formulations (Supplementary Figure 1) indicate that polymeric concentration has critical implications for bioink viscosity, and, consequently, the extrusion of the bioprints. In this study, the sodium alginate amount affects the homogeneity of the solution (Figure 1) in that too much sodium alginate will result in a heterogeneous ink that may significantly alter viscosity due to decreased solubility [128]. As increased temperature is applied to these bioinks with different polymeric concentrations, heat absorption leads to solubility increase resulting in lower viscosity (Supplementary Figure 1). However, the 10:2 gelatin alginate formulation demonstrated superior printing resolution and optimum viscosity for bioprinting compared to the formulations tested (Figure 1). Results from this study are further in agreement with rheological studies conducted by other groups that suggest that viscosity behavior as a function of temperature defines gelatin alginate as a thermosensitive polymer. Its controlled extrusion through fine needles, while maintaining fidelity in shape, indicates that the bioink acts as a non-Newtonian shear thinning fluid [69, 129–132]. These characteristics contribute to the ability to print fine architectures without compromising cell viability when shear rate changes. In addition to retaining shape fidelity, rheology of bioink dictates proliferation and spreading of living cells in the matrix [133]. Different formulations, including in this study and others[94, 130, 134, 135] were

shown to have substantial changes in viscosity as function of temperature and concentration, validating the utility of the 10:2 gelatin alginate formulation for bioprinting.

Another component in maintaining scaffold integrity is the crosslinking method. Bioprinted scaffolds were evaluated using different crosslinkers and crosslinking durations to assess the mechanical integrity of the scaffold over 28 d. Genipin and $CaCl_2$ are known to crosslink gelatin and sodium alginate, respectively [99, 102, 103, 136]; however, in this study, crosslinking with genipin-only resulted in compromised structural integrity by 7 d (Figure 3A). Similarly, $CaCl_2$-only scaffolds rapidly degraded within 8 hr (not shown). For dual-crosslinked scaffolds, it was observed that crosslinking for 24 hr, maintained the highest level of scaffold integrity over 28 d, both visually and with 13% less mass loss than scaffolds crosslinked with genipin-only (Figure 3B). These results suggest that dual-crosslinked scaffolds likely require longer crosslinking times to fully harden, and to maintain their shape for longer durations. Although the measurements and visual evidence are temporally consistent, it is acknowledged that scaffold degradation and swelling measurements may be affected by the proliferation of *L. crispatus* within them.

In parallel with mass loss studies, the swelling of dual-crosslinked scaffolds was assessed (Figure 3C). The dual-crosslinked scaffolds retained more of their initial mass relative to genipin-only crosslinked scaffolds. However, volumetric measurements were difficult to conduct due to minute changes in scaffold thicknesses and diameters. These data suggest that the scaffolds absorb minimal amounts of surrounding fluid (here, SVF). Minute changes to the gelatin alginate demonstrate how the matrix is advantageous for delivery of bacteria, whereas materials such as hydrogels are susceptible to absorption of vaginal secretions that alters release to initial bursts contingent on hydrogel polymer concentration [137]. The outcomes of scaffold degradation observed in this study provide support for the need of dual-crosslinking strategies for bioprinted gelatin alginate constructs, as also observed with osteoblast cells encapsulated in gelatin alginate [138]. Scaffolds that were not dual-crosslinked were more susceptible to degradation from interactions between sodium alginate and SVF; sodium alginate molecules would be expected to diffuse to the surface of the scaffold, causing, partial degradation as observed previously in gelatin alginate 3D-printing studies [139]. Figure 3B shows an initial degradation independent of crosslinking conditions that is likely driven by the lower pH of SVF. In contrast, Figure 4F shows a decrease in pH driven by the bacteria (scaffold evaluated in MRS). Over a longer time, scaffolds crosslinked with genipin-only did not retain shape fidelity and appeared to be more flattened, a phenomenon similarly observed with alginate particles after exposure to lower pH [140].

Cells incorporated via bioprinting are often susceptible to a logarithmic-scale reduction in viability, due to shear stress during the extrusion process[67, 129]. Given this, the post-print viability was evaluated to assess the effect of shear stress and temperature, resulting from the extrusion process (Figure 4A). Relative to the unprinted bioink, *L. crispatus* could be viably recovered from all inclusion concentrations and curing durations. Furthermore, a macrostructural evaluation of blank and *L. crispatus*-containing scaffolds showed scaffold integrity after immersion in SVF for 28 d (Figure 4B), further emphasizing the formulation selection and ability to bioprint *L. crispatus*-containing scaffolds with similar processing

parameters to blank scaffolds. When release and proliferation were taken together, at least 1 to 4×10^8 CFU of daily *L. crispatus* per mg scaffold was observed through 28 d. These results indicate that *L. crispatus* maintained metabolic viability through 28 d (Figure 4D). These results are additionally supported by pH measurements. The release and proliferation were consistently maintained through 28 d. To provide alternative initial cumulative release and proliferation, the polymeric concentrations as well as the bioprinted geometrics and infill distancing could be modified [141].

Additionally, production of D- and L-lactic acid was measured due to its antimicrobial and immunomodulatory properties. Lactic acid can compromise the viability of many pathogens by creating weak acid stress. Vaginal epithelial cells, like all mammalian cells, produce mostly the L-lactic acid isomer with a minimal amount of D-lactic acid through the methylglyoxal pathway [142]. This study showed that both scaffolds produced high amounts of lactic acid with higher D-lactic acid levels. These findings were in accordance with previous studies reporting that *L. crispatus* produced higher D- to L-lactic acid isomer ratios relative to other species[143–146]. At a physiological concentration of 100 mM, lactic acid acts as a microbicide towards BV-associated bacteria and does not hinder the presence of beneficial lactobacilli [147–150]. The results indicate that lactic acid is produced by viable and metabolically active bacteria to provide sustained release and probiotic proliferation for 28 d, with pH modulation (Figure 4E–F), providing a strong proof of concept for the current design. Through the characterized combination of gelatin alginate to provide advantageous diffusion of nutrients, enhanced cell adhesion, and delivery of antimicrobials[151, 152], the release of lactic acid in the presence of pathogenic bacteria, such as *G. vaginalis* is expected to acidify and affect intracellular function [150], lowering the potential of these pathogens to exploit the biomaterial matrix for their own proliferation and viability. Similarly, poly(hexamethylene biguanide) hydrochloride, an antibacterial, and hyaluronic acid multilayer film were incorporated into a gelatin alginate sponge where the antibacterial effects were evident as observed with the zone of inhibition[153].

In addition to assessing probiotic viability and release immediately post-print, the viability and release of probiotics after storage in different conditions was evaluated (Figure 5). *L. crispatus* remained viable after 4 wk storage at −20°C, storage at 4°C led to a reduction in apparent viability relative to fresh scaffolds, and scaffolds stored at room temperature resulted in non-viable bacteria. These results are consistent with previous observations with *L. crispatus*-containing gelling mucoadhesive hydrogels[64], New methods could be considered to improve viability in non-cold chain storage conditions; thermostability may be improved by encapsulating probiotic into the core of the scaffold, a method similarly used to fabricate electrospun fibers[154]. Via incorporation of *Lactobacillus rhamnosus* into 3D-bioprinted structures, improved probiotic viability was demonstrated in a simulated gastrointestinal environment [85]. Compared to *L. crispatus*, the superior thermotolerance of *Lactobacillus rhamnosus* makes it suitable for food applications [155, 156].

The fabrication and distribution of *L. crispatus* into the core of the scaffold is confirmed by cross-sectional SEM images (Supplementary Figure 3); the presence of *L. crispatus*, seen throughout the scaffold cross-section, provides support for viable proliferation throughout the scaffold, potentially relating to the consistency observed in daily release. Congruent with

macrostructural images (Figure 3 and Figure 4), dual-crosslinking may help to protect the scaffold from degradation and likely has a role in retaining probiotic viability. Viability may be improved in room temperature storage by using additives, such as xylitol, whey protein, sucrose fatty acid esters, and magnesium stearate, as shown in previous thermostability studies[157, 158].

While crosslinking is necessary to maintain the mechanical integrity of gelatin alginate scaffolds, it can be challenging to find crosslinkers that exert minimal toxicity on prokaryotic and eukaryotic cells, in particular when cells are printed within scaffolds. Moreover, finding the ideal combination of bioink and crosslinker can be challenging and may compromise safety and mechanical integrity. While $CaCl_2$ has been found to be a cytocompatible crosslinker for alginate[99, 159], most current methods of gelatin crosslinking are cytotoxic. Notably, the most popular gelatin crosslinking reagent, glutaraldehyde, can be toxic if it is biodegraded and released in the body[160]. In comparison, genipin has been shown to be a safer alternative to improve the mechanical and thermal properties of gelatin, as well as prolong its degradation time[98]. Despite the relative safety of genipin, there have been some concerns regarding acute and dose-dependent toxicity[161]. For this reason, scaffolds crosslinked with a variety of crosslinking reagents were preliminarily tested for cytotoxicity after administration to vaginal epithelial cells (Figure 6). Negligible toxicity was observed after treatment with all groups, including genipin-crosslinked, indicating promise *in vitro* with the concentrations tested. To improve crosslinking formulations, lower genipin concentrations may be evaluated to increase the margin of safety.

Lastly, the dual-crosslinked, *L. crispatus*-scaffolds exhibited strong inhibition capabilities against *G. vaginalis* (Figure 7). In particular, *L. crispatus* supernatant from 3D-bioprinted scaffolds recovered after a prolonged duration of 7 d showed a statistically significant ($p \leq 0.05$) inhibition in logarithmic viability of *G. vaginalis* compared to 1 d, demonstrating the advantage of sustained delivery of *L. crispatus*. Inhibition of *G. vaginalis* further provides insight into the extent of viability reduction contingent on probiotic recovery and and lactic acid production.

Conclusion

This study highlights the potential of bioprinting to construct well-defined architectures for controlled release and proliferation of probiotics, with the goal of sustained, localized delivery in the female reproductive tract. For the first time, bioprinted, novel *L. crispatus*-containing scaffolds were developed with controllable, sustained release and proliferation of *L. crispatus* that exhibited antibacterial capabilities and demonstrated potent inhibition against *G. vaginalis*, the predominant species in the vaginal microbiome during BV. Controlled release and proliferation of *L. crispatus*, incorporated in gelatin alginate, provides a means to promote probiotics that can outcompete pathogens and could serve as a prophylactic measure against microbiome dysbiosis. Further, this work offers a framework to analyze fabrication and bioprinting with polymers and probiotics to achieve sustained delivery. The 10:2 gelatin alginate formulation, demonstrated fine printing resolution, in addition to mechanical integrity over 28 d. The results show that live *L. crispatus* can

be recovered from bioprinted scaffolds, maintaining viability through different curing and storage conditions. Furthermore, from the preliminary *in vitro* studies conducted here, vaginal cell viability was maintained, indicating the potential for 3D-bioprinted scaffolds to advance to *ex vivo* and *in vivo* studies. This study focused on the fabrication and characterization of 3D bioprints for sustained delivery and controlled release/proliferation of probiotics, with the longer term goal of vaginal application. Follow-up work will evaluate efficacy of these constructs, including inhibition of pathogenic bacteria such as *G. vaginalis in vivo*. This work represents a first step towards this goal, potentially offering a new alternative for sustained probiotic delivery for female genital tract applications.

Supplementary Material

Refer to Web version on PubMed Central for supplementary material.

ACKNOWLEDGEMENTS

This work was partially supported by National Institutes of Health / National Institute of Allergy and Infectious Diseases grant R01AI168475 (A. Lewis & H. Frieboes).

REFERENCES

[1]. Haahr T, Jensen JS, Thomsen L, Duus L, Rygaard K, Humaidan P, Abnormal vaginal microbiota may be associated with poor reproductive outcomes: a prospective study in IVF patients, Hum Reprod, 31 (2016) 795–803. [PubMed: 26911864]

[2]. Nasioudis D, Linhares IM, Ledger WJ, Witkin SS, Bacterial vaginosis: a critical analysis of current knowledge, Bjog, 124 (2017) 61–69. [PubMed: 27396541]

[3]. Peebles K, Velloza J, Balkus JE, McClelland RS, Barnabas RV, High Global Burden and Costs of Bacterial Vaginosis: A Systematic Review and Meta-Analysis, Sex Transm Dis, 46 (2019) 304–311. [PubMed: 30624309]

[4]. Machado D, Castro J, Palmeira-de-Oliveira A, Martinez-de-Oliveira J, Cerca N, Bacterial Vaginosis Biofilms: Challenges to Current Therapies and Emerging Solutions, Frontiers in microbiology, 6 (2015) 1528. [PubMed: 26834706]

[5]. Mastromarino P, Vitali B, Mosca L, Bacterial vaginosis: a review on clinical trials with probiotics, The new microbiologica, 36 (2013) 229–238. [PubMed: 23912864]

[6]. Menard JP, Antibacterial treatment of bacterial vaginosis: current and emerging therapies, International journal of women's health, 3 (2011) 295–305.

[7]. Verstraelen H, Vervaet C, Remon JP, Rationale and Safety Assessment of a Novel Intravaginal Drug-Delivery System with Sustained DL-Lactic Acid Release, Intended for Long-Term Protection of the Vaginal Microbiome, PloS one, 11 (2016) e0153441. [PubMed: 27093291]

[8]. Brotman RM, Klebanoff MA, Nansel TR, Yu KF, Andrews WW, Zhang J, Schwebke JR, Bacterial vaginosis assessed by gram stain and diminished colonization resistance to incident gonococcal, chlamydial, and trichomonal genital infection, The Journal of infectious diseases, 202 (2010) 1907–1915. [PubMed: 21067371]

[9]. Wiesenfeld HC, Hillier SL, Krohn MA, Landers DV, Sweet RL, Bacterial vaginosis is a strong predictor of Neisseria gonorrhoeae and Chlamydia trachomatis infection, Clin Infect Dis, 36 (2003) 663–668. [PubMed: 12594649]

[10]. Wiesenfeld HC, Hillier SL, Krohn MA, Amortegui AJ, Heine RP, Landers DV, Sweet RL, Lower genital tract infection and endometritis: insight into subclinical pelvic inflammatory disease, Obstetrics and gynecology, 100 (2002) 456–463. [PubMed: 12220764]

[11]. Watts DH, Krohn MA, Hillier SL, Eschenbach DA, Bacterial vaginosis as a risk factor for post-cesarean endometritis, Obstetrics and gynecology, 75 (1990) 52–58. [PubMed: 2296423]

[12]. Leitich H, Kiss H, Asymptomatic bacterial vaginosis and intermediate flora as risk factors for adverse pregnancy outcome, Best Pract Res Clin Obstet Gynaecol, 21 (2007) 375–390. [PubMed: 17241817]

[13]. Leitich H, Bodner-Adler B, Brunbauer M, Kaider A, Egarter C, Husslein P, Bacterial vaginosis as a risk factor for preterm delivery: a meta-analysis, Am J Obstet Gynecol, 189 (2003) 139–147. [PubMed: 12861153]

[14]. Silver HM, Sperling RS, St Clair PJ, Gibbs RS, Evidence relating bacterial vaginosis to intraamniotic infection, Am J Obstet Gynecol, 161 (1989) 808–812. [PubMed: 2782365]

[15]. DiGiulio DB, Diversity of microbes in amniotic fluid, Seminars in fetal & neonatal medicine, 17 (2012) 2–11. [PubMed: 22137615]

[16]. DiGiulio DB, Romero R, Kusanovic JP, Gomez R, Kim CJ, Seok KS, Gotsch F, Mazaki-Tovi S, Vaisbuch E, Sanders K, Bik EM, Chaiworapongsa T, Oyarzun E, Relman DA, Prevalence and diversity of microbes in the amniotic fluid, the fetal inflammatory response, and pregnancy outcome in women with preterm pre-labor rupture of membranes, Am J Reprod Immunol, 64 (2010) 38–57. [PubMed: 20331587]

[17]. Berardi-Grassias L, Roy O, Berardi JC, Furioli J, Neonatal meningitis due to Gardnerella vaginalis, European journal of clinical microbiology & infectious diseases : official publication of the European Society of Clinical Microbiology, 7 (1988) 406–407. [PubMed: 3137044]

[18]. Hillier SL, Martius J, Krohn M, Kiviat N, Holmes KK, Eschenbach DA, A case-control study of chorioamnionic infection and histologic chorioamnionitis in prematurity, The New England journal of medicine, 319 (1988) 972–978. [PubMed: 3262199]

[19]. Holst E, Goffeng AR, Andersch B, Bacterial vaginosis and vaginal microorganisms in idiopathic premature labor and association with pregnancy outcome, Journal of clinical microbiology, 32 (1994) 176–186. [PubMed: 8126176]

[20]. Goldenberg RL, Klebanoff MA, Nugent R, Krohn MA, Hillier S, Andrews WW, Bacterial colonization of the vagina during pregnancy in four ethnic groups. Vaginal Infections and Prematurity Study Group, Am J Obstet Gynecol, 174 (1996) 1618–1621. [PubMed: 9065140]

[21]. Rezeberga D, Lazdane G, Kroica J, Sokolova L, Donders GG, Placental histological inflammation and reproductive tract infections in a low risk pregnant population in Latvia, Acta Obstet Gynecol Scand, 87 (2008) 360–365. [PubMed: 18307078]

[22]. Svare JA, Schmidt H, Hansen BB, Lose G, Bacterial vaginosis in a cohort of Danish pregnant women: prevalence and relationship with preterm delivery, low birthweight and perinatal infections, Bjog, 113 (2006) 1419–1425. [PubMed: 17010117]

[23]. Zhang X, Xu X, Li J, Li N, Yan T, Ju X, [Relationship between vaginal sialidase bacteria vaginosis and chorioammionitis], Zhonghua fu chan ke za zhi, 37 (2002) 588–590. [PubMed: 12487930]

[24]. Hitti J, Hillier SL, Agnew KJ, Krohn MA, Reisner DP, Eschenbach DA, Vaginal indicators of amniotic fluid infection in preterm labor, Obstetrics and gynecology, 97 (2001) 211–219. [PubMed: 11165584]

[25]. MacPhee RA, Hummelen R, Bisanz JE, Miller WL, Reid G, Probiotic strategies for the treatment and prevention of bacterial vaginosis, Expert Opin Pharmacother, 11 (2010) 2985–2995. [PubMed: 21080853]

[26]. Cohen CR, Wierzbicki MR, French AL, Morris S, Newmann S, Reno H, Green L, Miller S, Powell J, Parks T, Hemmerling A, Randomized Trial of Lactin-V to Prevent Recurrence of Bacterial Vaginosis, The New England journal of medicine, 382 (2020) 1906–1915. [PubMed: 32402161]

[27]. Machado D, Castro J, Palmeira-de-Oliveira A, Martinez-de-Oliveira J, Cerca N, Bacterial Vaginosis Biofilms: Challenges to Current Therapies and Emerging Solutions, Front Microbiol, 6 (2015) 1528. [PubMed: 26834706]

[28]. Bradshaw CS, Morton AN, Hocking J, Garland SM, Morris MB, Moss LM, Horvath LB, Kuzevska I, Fairley CK, High recurrence rates of bacterial vaginosis over the course of 12 months after oral metronidazole therapy and factors associated with recurrence, The Journal of infectious diseases, 193 (2006) 1478–1486. [PubMed: 16652274]

[29]. Vodstrcil LA, Muzny CA, Plummer EL, Sobel JD, Bradshaw CS, Bacterial vaginosis: drivers of recurrence and challenges and opportunities in partner treatment, BMC Medicine, 19 (2021). [PubMed: 33430856]

[30]. Punzón-Jiménez P, Labarta E, The impact of the female genital tract microbiome in women health and reproduction: a review, Journal of Assisted Reproduction and Genetics, 38 (2021) 2519–2541. [PubMed: 34110573]

[31]. Borges S, Silva J, Teixeira P, The role of lactobacilli and probiotics in maintaining vaginal health, Archives of Gynecology and Obstetrics, 289 (2014) 479–489. [PubMed: 24170161]

[32]. Recine N, Palma E, Domenici L, Giorgini M, Imperiale L, Sassu C, Musella A, Marchetti C, Muzii L, Benedetti Panici P, Restoring vaginal microbiota: biological control of bacterial vaginosis. A prospective case–control study using *Lactobacillus rhamnosus* BMX 54 as adjuvant treatment against bacterial vaginosis, Archives of Gynecology and Obstetrics, 293 (2016) 101–107. [PubMed: 26142892]

[33]. Chandrashekhar P, Minooei F, Arreguin W, Masigol M, Steinbach-Rankins JM, Perspectives on Existing and Novel Alternative Intravaginal Probiotic Delivery Methods in the Context of Bacterial Vaginosis Infection, The AAPS Journal, 23 (2021). [PubMed: 33417061]

[34]. Wang Z, He Y, Zheng Y, Probiotics for the Treatment of Bacterial Vaginosis: A Meta-Analysis, International Journal of Environmental Research and Public Health, 16 (2019) 3859. [PubMed: 31614736]

[35]. Wijgert J, Verwijs M, Lactobacilli-containing vaginal probiotics to cure or prevent bacterial or fungal vaginal dysbiosis: a systematic review and recommendations for future trial designs, BJOG: An International Journal of Obstetrics & Gynaecology, 127 (2020) 287–299. [PubMed: 31299136]

[36]. Palmeira-de-Oliveira R, Palmeira-de-Oliveira A, Martinez-de-Oliveira J, New strategies for local treatment of vaginal infections, Adv Drug Deliv Rev, 92 (2015) 105–122. [PubMed: 26144995]

[37]. Muzny CA, Kardas P, A Narrative Review of Current Challenges in the Diagnosis and Management of Bacterial Vaginosis, Sex Transm Dis, 47 (2020) 441–446. [PubMed: 32235174]

[38]. Faught BM, Reyes S, Characterization and Treatment of Recurrent Bacterial Vaginosis, J Womens Health (Larchmt), 28 (2019) 1218–1226. [PubMed: 31403349]

[39]. Coudray MS, Madhivanan P, Bacterial vaginosis-A brief synopsis of the literature, Eur J Obstet Gynecol Reprod Biol, 245 (2020) 143–148. [PubMed: 31901667]

[40]. Bohbot JM, Daraï E, Bretelle F, Brami G, Daniel C, Cardot JM, Efficacy and safety of vaginally administered lyophilized *Lactobacillus crispatus* IP 174178 in the prevention of bacterial vaginosis recurrence, J Gynecol Obstet Hum Reprod, 47 (2018) 81–86. [PubMed: 29196153]

[41]. Cianci A, Cicinelli E, De Leo V, Fruzzetti F, Massaro MG, Bulfoni A, Parazzini F, Perino A, Observational prospective study on *Lactobacillus plantarum* P 17630 in the prevention of vaginal infections, during and after systemic antibiotic therapy or in women with recurrent vaginal or genitourinary infections, J Obstet Gynaecol, 38 (2018) 693–696. [PubMed: 29526145]

[42]. Ngugi BM, Hemmerling A, Bukusi EA, Kikuvi G, Gikunju J, Shiboski S, Fredricks DN, Cohen CR, Effects of bacterial vaginosis-associated bacteria and sexual intercourse on vaginal colonization with the probiotic *Lactobacillus crispatus* CTV-05, Sex Transm Dis, 38 (2011) 1020–1027. [PubMed: 21992977]

[43]. Tomás M, Palmeira-de-Oliveira A, Simões S, Martinez-de-Oliveira J, Palmeira-de-Oliveira R, Bacterial vaginosis: Standard treatments and alternative strategies, Int J Pharm, 587 (2020) 119659. [PubMed: 32687973]

[44]. Homayouni A, Bastani P, Ziyadi S, Mohammad-Alizadeh-Charandabi S, Ghalibaf M, Mortazavian AM, Mehrabany EV, Effects of probiotics on the recurrence of bacterial vaginosis: a review, Journal of lower genital tract disease, 18 (2014) 79–86. [PubMed: 24299970]

[45]. Mastromarino P, Macchia S, Meggiorini L, Trinchieri V, Mosca L, Perluigi M, Midulla C, Effectiveness of *Lactobacillus*-containing vaginal tablets in the treatment of symptomatic bacterial vaginosis, Clin Microbiol Infect, 15 (2009) 67–74. [PubMed: 19046169]

[46]. Mohammed L, Javed M, Althwanay A, Ahsan F, Oliveri F, Goud HK, Mehkari Z, Rutkofsky IH, Live Bacteria Supplementation as Probiotic for Managing Fishy, Odorous Vaginal Discharge

Disease of Bacterial Vaginosis: An Alternative Treatment Option?, Cureus, 12 (2020) e12362. [PubMed: 33527045]

[47]. Tidbury FD, Langhart A, Weidlinger S, Stute P, Non-antibiotic treatment of bacterial vaginosis—a systematic review, Archives of Gynecology and Obstetrics, 303 (2021) 37–45. [PubMed: 33025086]

[48]. Mizgier M, Jarzabek-Bielecka G, Mruczyk K, Kedzia W, The role of diet and probiotics in prevention and treatment of bacterial vaginosis and vulvovaginal candidiasis in adolescent girls and non-pregnant women, Ginekologia Polska, 91 (2020) 412–416. [PubMed: 32779162]

[49]. Larsson PG, Stray-Pedersen B, Ryttig KR, Larsen S, Human lactobacilli as supplementation of clindamycin to patients with bacterial vaginosis reduce the recurrence rate; a 6-month, double-blind, randomized, placebo-controlled study, BMC Womens Health, 8 (2008) 3. [PubMed: 18197974]

[50]. Rodrigues F, et al. , Vaginal suppositories containing *Lactobacillus acidophilus*: development and characterization, Drug Development and Industrial Pharmacy, 41 (2015) 1518. [PubMed: 25265366]

[51]. Petricevic L, Witt A, The role of *Lactobacillus casei rhamnosus* Lcr35 in restoring the normal vaginal flora after antibiotic treatment of bacterial vaginosis, Bjog, 115 (2008) 1369–1374. [PubMed: 18823487]

[52]. Lai SK, Wang YY, Hida K, Cone R, Hanes J, Nanoparticles reveal that human cervicovaginal mucus is riddled with pores larger than viruses, Proceedings of the National Academy of Sciences of the United States of America, 107 (2010) 598–603. [PubMed: 20018745]

[53]. Ensign LM, Cone R, Hanes J, Nanoparticle-based drug delivery to the vagina: a review, Journal of controlled release : official journal of the Controlled Release Society, 190 (2014) 500–514. [PubMed: 24830303]

[54]. Baelo A, Levato R, Julian E, Crespo A, Astola J, Gavalda J, Engel E, Mateos-Timoneda MA, Torrents E, Disassembling bacterial extracellular matrix with DNase-coated nanoparticles to enhance antibiotic delivery in biofilm infections, Journal of controlled release : official journal of the Controlled Release Society, 209 (2015) 150–158. [PubMed: 25913364]

[55]. Bartley JB, Ferris DG, Allmond LM, Dickman ED, Dias JK, Lambert J, Personal digital assistants used to document compliance of bacterial vaginosis treatment, Sex Transm Dis, 31 (2004) 488–491. [PubMed: 15273582]

[56]. Chee WJY, Chew SY, Than LTL, Vaginal microbiota and the potential of Lactobacillus derivatives in maintaining vaginal health, Microbial Cell Factories, 19 (2020). [PubMed: 32013957]

[57]. Gunawardana M, Mullen M, Yoo J, Webster P, Moss JA, Baum MM, Sustained delivery of commensal bacteria from pod-intravaginal rings, Antimicrob Agents Chemother, 58 (2014) 2262–2267. [PubMed: 24492360]

[58]. Vuotto C, Longo F, Donelli G, Probiotics to counteract biofilm-associated infections: promising and conflicting data, International Journal of Oral Science, 6 (2014) 189–194. [PubMed: 25257882]

[59]. Cheow WS, Hadinoto K, Biofilm-like *Lactobacillus rhamnosus* probiotics encapsulated in alginate and carrageenan microcapsules exhibiting enhanced thermotolerance and freeze-drying resistance, Biomacromolecules, 14 (2013) 3214–3222. [PubMed: 23985031]

[60]. Jones SE, Versalovic J, Probiotic *Lactobacillus reuteri* biofilms produce antimicrobial and anti-inflammatory factors, BMC Microbiology, 9 (2009) 35. [PubMed: 19210794]

[61]. Asvadi NH, Dang NT, Davis-Poynter N, Coombes AG, Evaluation of microporous polycaprolactone matrices for controlled delivery of antiviral microbicides to the female genital tract, J Mater Sci Mater Med, 24 (2013) 2719–2727. [PubMed: 23892484]

[62]. Baum MM, Butkyavichene I, Gilman J, Kennedy S, Kopin E, Malone AM, Nguyen C, Smith TJ, Friend DR, Clark MR, Moss JA, An intravaginal ring for the simultaneous delivery of multiple drugs, J Pharm Sci, 101 (2012) 2833–2843. [PubMed: 22619076]

[63]. Rençber S, Karavana SY, Şenyiğit ZA, Eraç B, Limoncu MH, Baloğlu E, Mucoadhesive in situ gel formulation for vaginal delivery of clotrimazole: formulation, preparation, and in vitro/in vivo evaluation, Pharm Dev Technol, 22 (2017) 551–561. [PubMed: 27055376]

[64]. Gnaman KNG, et al. , Characterization and in vitro evaluation of a vaginal gel containing *Lactobacillus crispatus* for the prevention of gonorrhea, International Journal of Pharmaceutics, 588 (2020) 119733. [PubMed: 32768529]

[65]. Vigani Faccendini, Rossi Sandri, Bonferoni Grisoli, Ferrari, Development of a Mucoadhesive in Situ Gelling Formulation for the Delivery of *Lactobacillus gasseri* into Vaginal Cavity, Pharmaceutics, 11 (2019) 511. [PubMed: 31623341]

[66]. Zhao Y, Wang T, Chen Z, Ren H, Song P, Zhu Y, Liang S, Tzeng C, Development and Evaluation of a Thermosensitive In Situ Gel Formulation for Intravaginal Delivery of Lactobacillus gasseri, Pharmaceutics, 14 (2022) 1934. [PubMed: 36145685]

[67]. Emmermacher J, Spura D, Cziommer J, Kilian D, Wollborn T, Fritsching U, Steingroewer J, Walther T, Gelinsky M, Lode A, Engineering considerations on extrusion-based bioprinting: interactions of material behavior, mechanical forces and cells in the printing needle, Biofabrication, 12 (2020) 025022. [PubMed: 32050179]

[68]. Matai I, Kaur G, Seyedsalehi A, McClinton A, Laurencin CT, Progress in 3D bioprinting technology for tissue/organ regenerative engineering, Biomaterials, 226 (2020) 119536. [PubMed: 31648135]

[69]. Rastogi P, Kandasubramanian B, Review of alginate-based hydrogel bioprinting for application in tissue engineering, Biofabrication, 11 (2019) 042001. [PubMed: 31315105]

[70]. Liu P, Shen H, Zhi Y, Si J, Shi J, Guo L, Shen SG, 3D bioprinting and in vitro study of bilayered membranous construct with human cells-laden alginate/gelatin composite hydrogels, Colloids Surf B Biointerfaces, 181 (2019) 1026–1034. [PubMed: 31382330]

[71]. Chen Q, Tian X, Fan J, Tong H, Ao Q, Wang X, An Interpenetrating Alginate/Gelatin Network for Three-Dimensional (3D) Cell Cultures and Organ Bioprinting, Molecules, 25 (2020) 756. [PubMed: 32050529]

[72]. Shi L, Xiong L, Hu Y, Li W, Chen Z, Liu K, Zhang X, Three-dimensional printing alginate/gelatin scaffolds as dermal substitutes for skin tissue engineering, Polymer Engineering & Science, 58 (2018) 1782–1790.

[73]. Salahuddin B, Wang S, Sangian D, Aziz S, Gu Q, Hybrid Gelatin Hydrogels in Nanomedicine Applications, ACS Applied Bio Materials, 4 (2021) 2886–2906.

[74]. Muthukrishnan L, Imminent antimicrobial bioink deploying cellulose, alginate, EPS and synthetic polymers for 3D bioprinting of tissue constructs, Carbohydr Polym, 260 (2021) 117774. [PubMed: 33712131]

[75]. Mirek A, Belaid H, Barranger F, Grzeczkowicz M, Bouden Y, Cavaillès V, Lewińska D, Bechelany M, Development of a new 3D bioprinted antibiotic delivery system based on a cross-linked gelatin–alginate hydrogel, Journal of Materials Chemistry B, 10 (2022) 8862–8874. [PubMed: 35980231]

[76]. Homem NC, Tavares TD, Miranda CS, Antunes JC, Amorim MTP, Felgueiras HP, Functionalization of Crosslinked Sodium Alginate/Gelatin Wet-Spun Porous Fibers with Nisin Z for the Inhibition of Staphylococcus aureus-Induced Infections, International Journal of Molecular Sciences, 22 (2021) 1930. [PubMed: 33669209]

[77]. Mohammadi Z, Rabbani M, Bacterial Bioprinting on a Flexible Substrate for Fabrication of a Colorimetric Temperature Indicator by Using a Commercial Inkjet Printer, J Med Signals Sens, 8 (2018) 170–174. [PubMed: 30181965]

[78]. Dubbin K, Dong Z, Park DM, Alvarado J, Su J, Wasson E, Robertson C, Jackson J, Bose A, Moya ML, Jiao Y, Hynes WF, Projection Microstereolithographic Microbial Bioprinting for Engineered Biofilms, Nano Letters, 21 (2021) 1352–1359. [PubMed: 33508203]

[79]. Lehner BAE, Schmieden DT, Meyer AS, A Straightforward Approach for 3D Bacterial Printing, ACS Synth Biol, 6 (2017) 1124–1130. [PubMed: 28225616]

[80]. Rodríguez-Dévora JI, Zhang B, Reyna D, Shi Z-D, Xu T, High throughput miniature drug-screening platform using bioprinting technology, Biofabrication, 4 (2012) 035001. [PubMed: 22728820]

[81]. Ning E, Turnbull G, Clarke J, Picard F, Riches P, Vendrell M, Graham D, Wark AW, Faulds K, Shu W, 3D bioprinting of mature bacterial biofilms for antimicrobial resistance drug testing, Biofabrication, 11 (2019) 045018. [PubMed: 31370051]

[82]. Schmieden DT, Basalo Vázquez SJ, Sangüesa H, van der Does M, Idema T, Meyer AS, Printing of Patterned, Engineered E. coli Biofilms with a Low-Cost 3D Printer, ACS Synth Biol, 7 (2018) 1328–1337. [PubMed: 29690761]

[83]. Balasubramanian S, Aubin-Tam ME, Meyer AS, 3D Printing for the Fabrication of Biofilm-Based Functional Living Materials, ACS Synth Biol, 8 (2019) 1564–1567. [PubMed: 31319670]

[84]. Zhang L, Lou Y, Schutyser M, 3D printing of cereal-based food structures containing probiotics, Food Structure, 18 (2018) 14–22.

[85]. Mallick A, Quilès F, Francius G, Burgain J, Gaiani C, Scher J, Amara S, Lemaitre C, Marchal P, Alem H, An easy and robust method of preparation of capsules for delivering probiotic bacteria by a 3D bioprinting, Food Hydrocolloids for Health, 2 (2022) 100088.

[86]. Cui Z, Feng Y, Liu F, Jiang L, Yue J, 3D Bioprinting of Living Materials for Structure-Dependent Production of Hyaluronic Acid, ACS Macro Lett, 11 (2022) 452–459. [PubMed: 35575323]

[87]. Duraj-Thatte AM, Manjula-Basavanna A, Rutledge J, Xia J, Hassan S, Sourlis A, Rubio AG, Lesha A, Zenkl M, Kan A, Weitz DA, Zhang YS, Joshi NS, Programmable microbial ink for 3D printing of living materials produced from genetically engineered protein nanofibers, Nature Communications, 12 (2021).

[88]. Verstraelen H, Verhelst R, Claeys G, De Backer E, Temmerman M, Vaneechoutte M, Longitudinal analysis of the vaginal microflora in pregnancy suggests that *L. crispatus* promotes the stability of the normal vaginal microflora and that *L. gasseri* and/or *L. iners* are more conducive to the occurrence of abnormal vaginal microflora, BMC Microbiology, 9 (2009) 116. [PubMed: 19490622]

[89]. Tortelli BA, Lewis WG, Allsworth JE, Member-Meneh N, Foster LR, Reno HE, Peipert JF, Fay JC, Lewis AL, Associations between the vaginal microbiome and Candida colonization in women of reproductive age, Am J Obstet Gynecol, 222 (2020) 471.e471–471.e479.

[90]. Chen H, Min S, Wang L, Zhao L, Luo F, Lei W, Wen Y, Luo L, Zhou Q, Peng L, Li Z, *Lactobacillus* Modulates Chlamydia Infectivity and Genital Tract Pathology in vitro and in vivo, Front Microbiol, 13 (2022) 877223. [PubMed: 35572713]

[91]. Tietz K, Klein S, Simulated Genital Tract Fluids and Their Applicability in Drug Release/Dissolution Testing of Vaginal Dosage Forms, Dissolution Technologies, 25 (2018) 40–51.

[92]. Wu Z, Su X, Xu Y, Kong B, Sun W, Mi S, Bioprinting three-dimensional cell-laden tissue constructs with controllable degradation, Sci Rep, 6 (2016) 24474. [PubMed: 27091175]

[93]. Huang S, Yao B, Xie J, Fu X, 3D bioprinted extracellular matrix mimics facilitate directed differentiation of epithelial progenitors for sweat gland regeneration, Acta Biomater, 32 (2016) 170–177. [PubMed: 26747979]

[94]. Duan B, Hockaday LA, Kang KH, Butcher JT, 3D bioprinting of heterogeneous aortic valve conduits with alginate/gelatin hydrogels, J Biomed Mater Res A, 101 (2013) 1255–1264. [PubMed: 23015540]

[95]. Li Z, Huang S, Liu Y, Yao B, Hu T, Shi H, Xie J, Fu X, Tuning Alginate-Gelatin Bioink Properties by Varying Solvent and Their Impact on Stem Cell Behavior, Scientific Reports, 8 (2018). [PubMed: 29311689]

[96]. Mahjabeen S, Hatipoglu MK, Chandra V, Benbrook DM, Garcia-Contreras L, Optimization of a Vaginal Suppository Formulation to Deliver SHetA2 as a Novel Treatment for Cervical Dysplasia, Journal of Pharmaceutical Sciences, 107 (2018) 638–646. [PubMed: 28989018]

[97]. Muzzarelli RA, El Mehtedi M, Bottegoni C, Aquili A, Gigante A, Genipin-Crosslinked Chitosan Gels and Scaffolds for Tissue Engineering and Regeneration of Cartilage and Bone, Mar Drugs, 13 (2015) 7314–7338. [PubMed: 26690453]

[98]. Bigi A, Cojazzi G, Panzavolta S, Roveri N, Rubini K, Stabilization of gelatin films by crosslinking with genipin, Biomaterials, 23 (2002) 4827–4832. [PubMed: 12361622]

[99]. Saarai A, Kbapárková V, Sedlacek T, Sáha P, A comparative study of crosslinked sodium alginate/gelatin hydrogels for wound dressing, in, 2011.

[100]. Seixas FL, Turbiani F, Salomao PG, Souza RP, Gimenes ML, Biofilms Composed of Alginate and Pectin: Effect of Concentration of Crosslinker and Plasticizer Agents, Chemical engineering transactions, 32 (2013) 1693–1698.

[101]. Hariyadi D, Hendradi E, Purwanti T, Fadil FDGP, Ramadani CN, Effect of cross linking agent and polymer on the characteristics of ovalbumin loaded alginate microspheres, International Journal of Pharmacy and Pharmaceutical Sciences, 6 (2014) 469–474.

[102]. Ma W, Yin S-W, Yang X-Q, Qi J-R, Genipin-crosslinked gelatin films as controlled releasing carriers of lysozyme, Food Research International, 51 (2013) 321–324.

[103]. Gorczyca G, Tylingo R, Szweda P, Augustin E, Sadowska M, Milewski S, Preparation and characterization of genipin cross-linked porous chitosan-collagen-gelatin scaffolds using chitosan-CO2 solution, Carbohydr Polym, 102 (2014) 901–911. [PubMed: 24507362]

[104]. Mitchell C, Paul K, Agnew K, Gaussman R, Coombs RW, Hitti J, Estimating Volume of Cervicovaginal Secretions in Cervicovaginal Lavage Fluid Collected for Measurement of Genital HIV-1 RNA Levels in Women, Journal of Clinical Microbiology, 49 (2011) 735–736. [PubMed: 21106793]

[105]. Owen DH, Katz DF, A vaginal fluid simulant, Contraception, 59 (1999) 91–95. [PubMed: 10361623]

[106]. Oh J, Kim B, Mucoadhesive and pH-responsive behavior of gelatin containing hydrogels for protein drug delivery applications, Korea-Australia Rheology Journal, 32 (2020) 41.

[107]. Dos Santos AM, Carvalho SG, Araujo VHS, Carvalho GC, Gremião MPD, Chorilli M, Recent advances in hydrogels as strategy for drug delivery intended to vaginal infections, Int J Pharm, 590 (2020) 119867. [PubMed: 32919001]

[108]. Aroutcheva A, et al. , Defense factors of vaginal lactobacilli, American Journal of Obstetrics and Gynecology, 185 (2001) 375. [PubMed: 11518895]

[109]. Borchers AT, et al. , Probiotics and immunity, Journal of Gastroenterology, 44 (2009) 26. [PubMed: 19159071]

[110]. Gunawardana M, Baum MM, Smith TJ, Moss JA, An intravaginal ring for the sustained delivery of antibodies, J Pharm Sci, 103 (2014) 3611–3620. [PubMed: 25231193]

[111]. Yan WC, Davoodi P, Vijayavenkataraman S, Tian Y, Ng WC, Fuh JYH, Robinson KS, Wang CH, 3D bioprinting of skin tissue: From pre-processing to final product evaluation, Adv Drug Deliv Rev, 132 (2018) 270–295. [PubMed: 30055210]

[112]. Luis E, Pan HM, Sing SL, Bajpai R, Song J, Yeong WY, 3D Direct Printing of Silicone Meniscus Implant Using a Novel Heat-Cured Extrusion-Based Printer, Polymers (Basel), 12 (2020). [PubMed: 33375138]

[113]. Shapira A, Dvir T, 3D Tissue and Organ Printing—Hope and Reality, Advanced Science, 8 (2021) 2003751. [PubMed: 34026444]

[114]. Gu Z, et al. , Development of 3D bioprinting: From printing methods to biomedical applications, Asian Journal of Pharmaceutical Sciences, 15 (2020) 529. [PubMed: 33193859]

[115]. Gungor-Ozkerim PS, Inci I, Zhang YS, Khademhosseini A, Dokmeci MR, Bioinks for 3D bioprinting: an overview, Biomaterials Science, 6 (2018) 915–946. [PubMed: 29492503]

[116]. Connell JL, et al. , 3D printing of microscopic bacterial communities, Proceedings of the National Academy of Sciences of the United States of America, 110 (2013) 18380. [PubMed: 24101503]

[117]. Joshi S, Cook E, Mannoor MS, Bacterial Nanobionics via 3D Printing, Nano Lett, 18 (2018) 7448–7456. [PubMed: 30403141]

[118]. Mandrycky C, Wang Z, Kim K, Kim DH, 3D bioprinting for engineering complex tissues, Biotechnol Adv, 34 (2016) 422–434. [PubMed: 26724184]

[119]. Zhang M, Zhuang B, Du G, Han G, Jin Y, Curcumin solid dispersion-loaded in situ hydrogels for local treatment of injured vaginal bacterial infection and improvement of vaginal wound healing, J Pharm Pharmacol, 71 (2019) 1044–1054. [PubMed: 30887519]

[120]. Sundara Rajan S, Cavera VL, Zhang X, Singh Y, Chikindas ML, Sinko PJ, Polyethylene Glycol-Based Hydrogels for Controlled Release of the Antimicrobial Subtilosin for Prophylaxis of Bacterial Vaginosis, Antimicrobial Agents and Chemotherapy, 58 (2014) 2747–2753. [PubMed: 24566190]

[121]. Schwartz R, Malpica M, Thompson GL, Miri AK, Cell encapsulation in gelatin bioink impairs 3D bioprinting resolution, J Mech Behav Biomed Mater, 103 (2020) 103524. [PubMed: 31785543]

[122]. Malcolm RK, et al. , Advances in microbicide vaginal rings, Antiviral Research, 88 (2010) 30.

[123]. Chachlioutaki K, Karavasili C, Mavrokefalou EE, Gioumouxouzis CI, Ritzoulis C, Fatouros DG, Quality control evaluation of paediatric chocolate-based dosage forms: 3D printing vs mold-casting method, Int J Pharm, 624 (2022) 121991. [PubMed: 35809833]

[124]. Suárez-González J, et al. , Individualized orodispersible pediatric dosage forms obtained by molding and semi-solid extrusion by 3D printing: A comparative study for hydrochlorothiazide, Journal of Drug Delivery Science and Technology, 66 (2021) 102884.

[125]. Paxton N, Smolan W, Böck T, Melchels F, Groll J, Jungst T, Proposal to assess printability of bioinks for extrusion-based bioprinting and evaluation of rheological properties governing bioprintability, Biofabrication, 9 (2017) 044107. [PubMed: 28930091]

[126]. Wüst S, Godla ME, Müller R, Hofmann S, Tunable hydrogel composite with two-step processing in combination with innovative hardware upgrade for cell-based three-dimensional bioprinting, Acta Biomaterialia, 10 (2014) 630–640. [PubMed: 24157694]

[127]. Augst AD, Kong HJ, Mooney DJ, Alginate Hydrogels as Biomaterials, Macromolecular Bioscience, 6 (2006) 623. [PubMed: 16881042]

[128]. Derkach SR, Kolotova DS, Voron'ko NG, Obluchinskaya ED, Malkin AY, Rheological Properties of Fish Gelatin Modified with Sodium Alginate, Polymers (Basel), 13 (2021). [PubMed: 35012038]

[129]. Gómez-Blanco JC, Mancha-Sánchez E, Marcos AC, Matamoros M, Díaz-Parralejo A, Pagador JB, Bioink Temperature Influence on Shear Stress, Pressure and Velocity Using Computational Simulation, Processes, 8 (2020) 865.

[130]. Ouyang L, Yao R, Zhao Y, Sun W, Effect of bioink properties on printability and cell viability for 3D bioplotting of embryonic stem cells, Biofabrication, 8 (2016) 035020. [PubMed: 27634915]

[131]. Gao T, Gillispie GJ, Copus JS, Pr AK, Seol Y-J, Atala A, Yoo JJ, Lee SJ, Optimization of gelatin–alginate composite bioink printability using rheological parameters: a systematic approach, Biofabrication, 10 (2018) 034106. [PubMed: 29923501]

[132]. Cooke ME, Rosenzweig DH, The rheology of direct and suspended extrusion bioprinting, APL Bioengineering, 5 (2021) 011502. [PubMed: 33564740]

[133]. Vignesh S, et al. , Fabrication of micropatterned alginate-gelatin and k-carrageenan hydrogels of defined shapes using simple wax mould method as a platform for stem cell/induced Pluripotent Stem Cells (iPSC) culture, International Journal of Biological Macromolecules, 112 (2018) 737. [PubMed: 29427684]

[134]. Bociaga D, Bartniak M, Grabarczyk J, Przybyszewska K, Sodium Alginate/Gelatine Hydrogels for Direct Bioprinting—The Effect of Composition Selection and Applied Solvents on the Bioink Properties, Materials, 12 (2019) 2669. [PubMed: 31443354]

[135]. Giuseppe MD, Law N, Webb B, R AM, Liew LJ, Sercombe TB, Dilley RJ, Doyle BJ, Mechanical behaviour of alginate-gelatin hydrogels for 3D bioprinting, J Mech Behav Biomed Mater, 79 (2018) 150–157. [PubMed: 29304429]

[136]. Erdagi SI, Ngwabebhoh FA, Yildiz U, Genipin crosslinked gelatin-diosgenin-nanocellulose hydrogels for potential wound dressing and healing applications, International Journal of Biological Macromolecules, 149 (2020) 651. [PubMed: 32006574]

[137]. Taurin S, Almomen AA, Pollak T, Kim SJ, Maxwell J, Peterson CM, Owen SC, Janát-Amsbury MM, Thermosensitive hydrogels a versatile concept adapted to vaginal drug delivery, J Drug Target, 26 (2018) 533–550. [PubMed: 29096548]

[138]. Chawla D, Kaur T, Joshi A, Singh N, 3D bioprinted alginate-gelatin based scaffolds for soft tissue engineering, Int J Biol Macromol, 144 (2020) 560–567. [PubMed: 31857163]

[139]. Curti F, Drăguşin DM, Serafim A, Iovu H, Stancu IC, Development of thick paste-like inks based on superconcentrated gelatin/alginate for 3D printing of scaffolds with shape fidelity and stability, Mater Sci Eng C Mater Biol Appl, 122 (2021) 111866. [PubMed: 33641888]

[140]. Chuang J-J, Huang Y-Y, Lo S-H, Hsu T-F, Huang W-Y, Huang S-L, Lin Y-S, Effects of pH on the Shape of Alginate Particles and Its Release Behavior, International Journal of Polymer Science, 2017 (2017) 1–9.

[141]. Olmos-Juste R, Guaresti O, Calvo-Correas T, Gabilondo N, Eceiza A, Design of drug-loaded 3D printing biomaterial inks and tailor-made pharmaceutical forms for controlled release, Int J Pharm, 609 (2021) 121124. [PubMed: 34597726]

[142]. Witkin SS, Mendes-Soares H, Linhares IM, Jayaram A, Ledger WJ, Forney LJ, Influence of vaginal bacteria and D- and L-lactic acid isomers on vaginal extracellular matrix metalloproteinase inducer: implications for protection against upper genital tract infections, mBio, 4 (2013).

[143]. Tachedjian G, Aldunate M, Bradshaw CS, Cone RA, The role of lactic acid production by probiotic *Lactobacillus* species in vaginal health, Research in microbiology, 168 (2017) 782–792. [PubMed: 28435139]

[144]. Witkin SS, Mendes-Soares H, Linhares IM, Jayaram A, Ledger WJ, Forney LJ, Influence of Vaginal Bacteria and d - and l -Lactic Acid Isomers on Vaginal Extracellular Matrix Metalloproteinase Inducer: Implications for Protection against Upper Genital Tract Infections, mBio, 4 (2013) e00460–00413-e00460. [PubMed: 23919998]

[145]. Borgogna J-LC, Shardell MD, Grace SG, Santori EK, Americus B, Li Z, Ulanov A, Forney L, Nelson TM, Brotman RM, Ravel J, Yeoman CJ, Biogenic Amines Increase the Odds of Bacterial Vaginosis and Affect the Growth of and Lactic Acid Production by Vaginal *Lactobacillus spp*, Applied and Environmental Microbiology, 87 (2021).

[146]. Abdelmaksoud AA, Koparde VN, Sheth NU, Serrano MG, Glascock AL, Fettweis JM, Strauss JF, Buck GA, Jefferson KK, Comparison of *Lactobacillus crispatus* isolates from *Lactobacillus*-dominated vaginal microbiomes with isolates from microbiomes containing bacterial vaginosis-associated bacteria, Microbiology, 162 (2016) 466–475. [PubMed: 26747455]

[147]. Hanlon DEO, Moench TR, Cone RA, In vaginal fluid, bacteria associated with bacterial vaginosis can be suppressed with lactic acid but not hydrogen peroxide, BMC Infectious Diseases, 11 (2011) 200. [PubMed: 21771337]

[148]. O'Hanlon DE, Come RA, Moench TR, Vaginal pH measured in vivo: lactobacilli determine pH and lactic acid concentration, BMC Microbiology, 19 (2019). [PubMed: 30665346]

[149]. Beghini J, Giraldo PC, Linhares IM, Ledger WJ, Witkin SS, Neutrophil Gelatinase-Associated Lipocalin Concentration in Vaginal Fluid, Reproductive Sciences, 22 (2015) 964–968. [PubMed: 25670719]

[150]. Tachedjian G, et al. , The role of lactic acid production by probiotic *Lactobacillus* species in vaginal health, Research in Microbiology, 168 (2017) 782. [PubMed: 28435139]

[151]. Ma H, Yu K, Wang H, Liu J, Cheng YY, Kang Y, Wang H, Zhang J, Song K, Fabrication and detection of a novel hybrid conductive scaffold based on alginate/gelatin/carboxylated carbon nanotubes (Alg/Gel/mMWCNTs) for neural tissue engineering, Tissue Cell, 80 (2023) 101995. [PubMed: 36512950]

[152]. Chen H, Song Y, Pen Y, Wang M, Dessie W, Duns GJ, Xu L, Luo X, Qin Z, Hydrogel Complex Containing the Antimicrobial Peptide HX-12C Accelerates Healing of Infected Wounds, Macromol Biosci, (2023) e2200514. [PubMed: 36662610]

[153]. Che C, Liu L, Wang X, Zhang X, Luan S, Yin J, Li X, Shi H, Surface-Adaptive and On-Demand Antibacterial Sponge for Synergistic Rapid Hemostasis and Wound Disinfection, ACS Biomaterials Science & Engineering, 6 (2020) 1776–1786. [PubMed: 33455385]

[154]. Feng K, et al. , Improved Viability and Thermal Stability of the Probiotics Encapsulated in a Novel Electrospun Fiber Mat, Journal of Agricultural and Food Chemistry, 66 (2018) 10890. [PubMed: 30260640]

[155]. Cheow WS, Hadinoto K, Biofilm-Like *Lactobacillus rhamnosus* Probiotics Encapsulated in Alginate and Carrageenan Microcapsules Exhibiting Enhanced Thermotolerance and Freeze-Drying Resistance, Biomacromolecules, 14 (2013) 3214–3222. [PubMed: 23985031]

[156]. Ananta E, Knorr D, Evidence on the role of protein biosynthesis in the induction of heat tolerance of *Lactobacillus rhamnosus* GG by pressure pre-treatment, Int J Food Microbiol, 96 (2004) 307–313. [PubMed: 15454321]

[157]. Kang M-S, Kim Y-S, Lee H-C, Lim H-S, Oh J-S, Comparison of Temperature and Additives Affecting the Stability of the ProbioticWeissella cibaria, Chonnam Medical Journal, 48 (2012) 159. [PubMed: 23323221]

[158]. Çaglar E, et al. , Effect of chewing gums containing xylitol or probiotic bacteria on salivary mutans streptococci and lactobacilli, Clinical Oral Investigations, 11 (2007) 425. [PubMed: 17574481]

[159]. Kuo CK, Ma PX, Maintaining dimensions and mechanical properties of ionically crosslinked alginate hydrogel scaffolds in vitro, J Biomed Mater Res A, 84 (2008) 899–907. [PubMed: 17647237]

[160]. Reddy N, Reddy R, Jiang Q, Crosslinking biopolymers for biomedical applications, Trends Biotechnol, 33 (2015) 362–369. [PubMed: 25887334]

[161]. Wang C, Lau TT, Loh WL, Su K, Wang DA, Cytocompatibility study of a natural biomaterial crosslinker--Genipin with therapeutic model cells, J Biomed Mater Res B Appl Biomater, 97 (2011) 58–65. [PubMed: 21381191]

Figure 1.

Representative images of gelatin alginate scaffolds bioprinted with different formulation ratios. Line prints of the 10:1, 10:2, 11:2, 12:2, and 16:4 w/v blank and *L. crispatus*-containing gelatin alginate formulations extruded at 42 psi and 37°C with a 30G needle, shown immediately post-print. Coded file line width was defined as 0.68 mm. The 10:2 ratio provided line resolutions closest to computer-aided design (CAD) drawing specifications for both the blank and *L. crispatus*-containing scaffolds. Scale bar represents 1 mm.

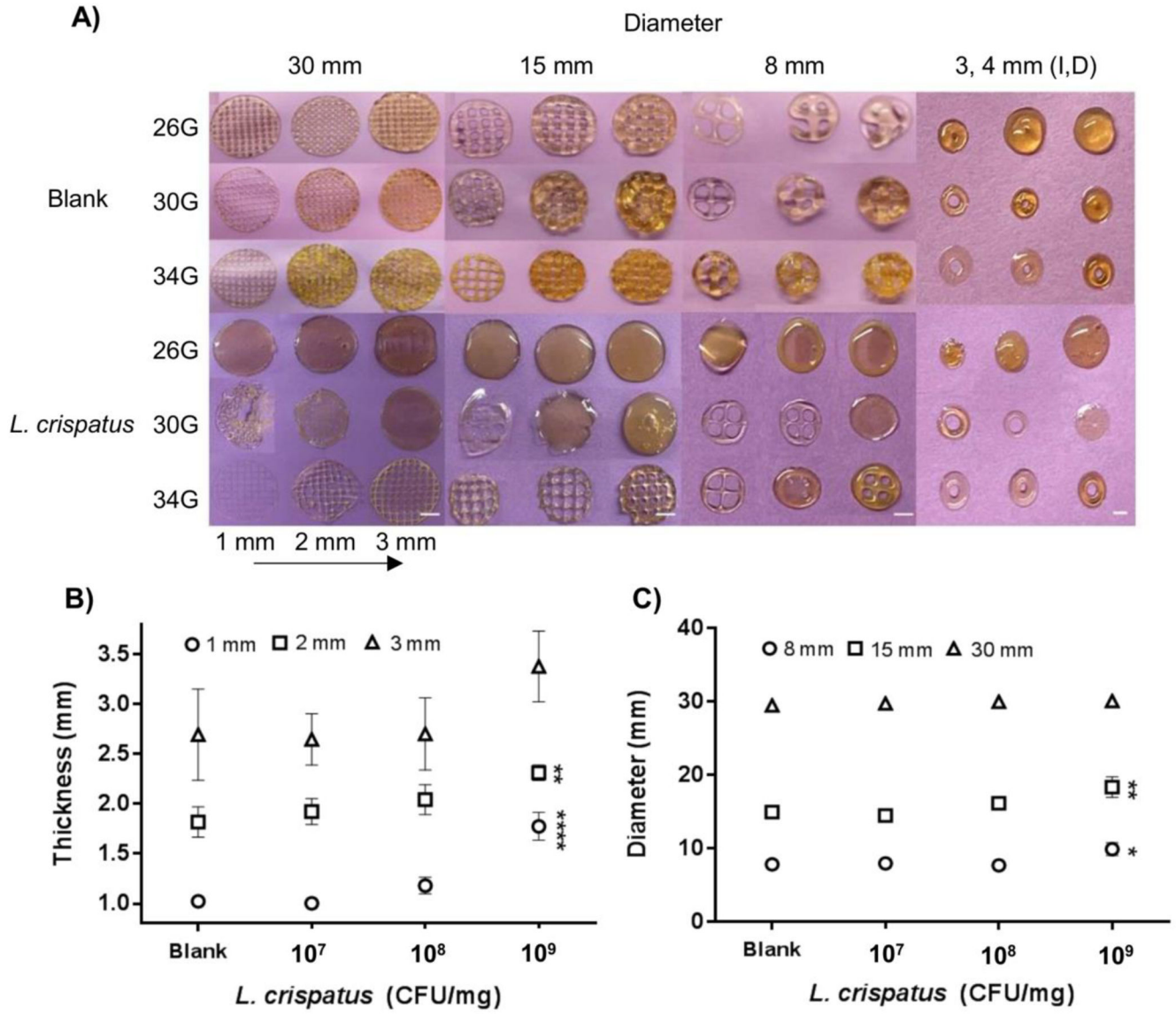

Figure 2.

Characterization of *L. crispatus*-containing scaffolds bioprinted using a 10:2 w/v gelatin alginate bioink. (A) Representative images from blank and *L. crispatus*-containing scaffolds printed using 26, 30, and 34G needles and extrusion pressure was adjusted to compensate for different needle gauges. Scaffolds were printed with 30, 15, and 8 mm diameters. Within each subpanel, the input thickness of printed scaffolds increased from 1 to 3 mm (left to right). Subpanels show blank and *L. crispatus*-containing ring structures fabricated with 3 and 4 mm inner (I) and outer diameter (D), respectively. Scale bars represent 10, 5, 3 and 2 mm from left to right. The reproducibility in (B) thickness and (C) diameter of blank and *L. crispatus*-containing scaffolds were measured as a function of probiotic incorporation. Panel B shows the measured thicknesses from 8 mm diameter scaffolds printed with 1, 2, and 3 mm thicknesses. Panel C shows the measured diameters from 1 mm thick scaffolds printed with 8, 15, and 30 mm diameters. Statistical significance between different concentration

groups and blank, as calculated by one-way ANOVA, is represented by *$p \leq 0.05$, ** $p \leq 0.01$ and ****$p \leq 0.0001$.

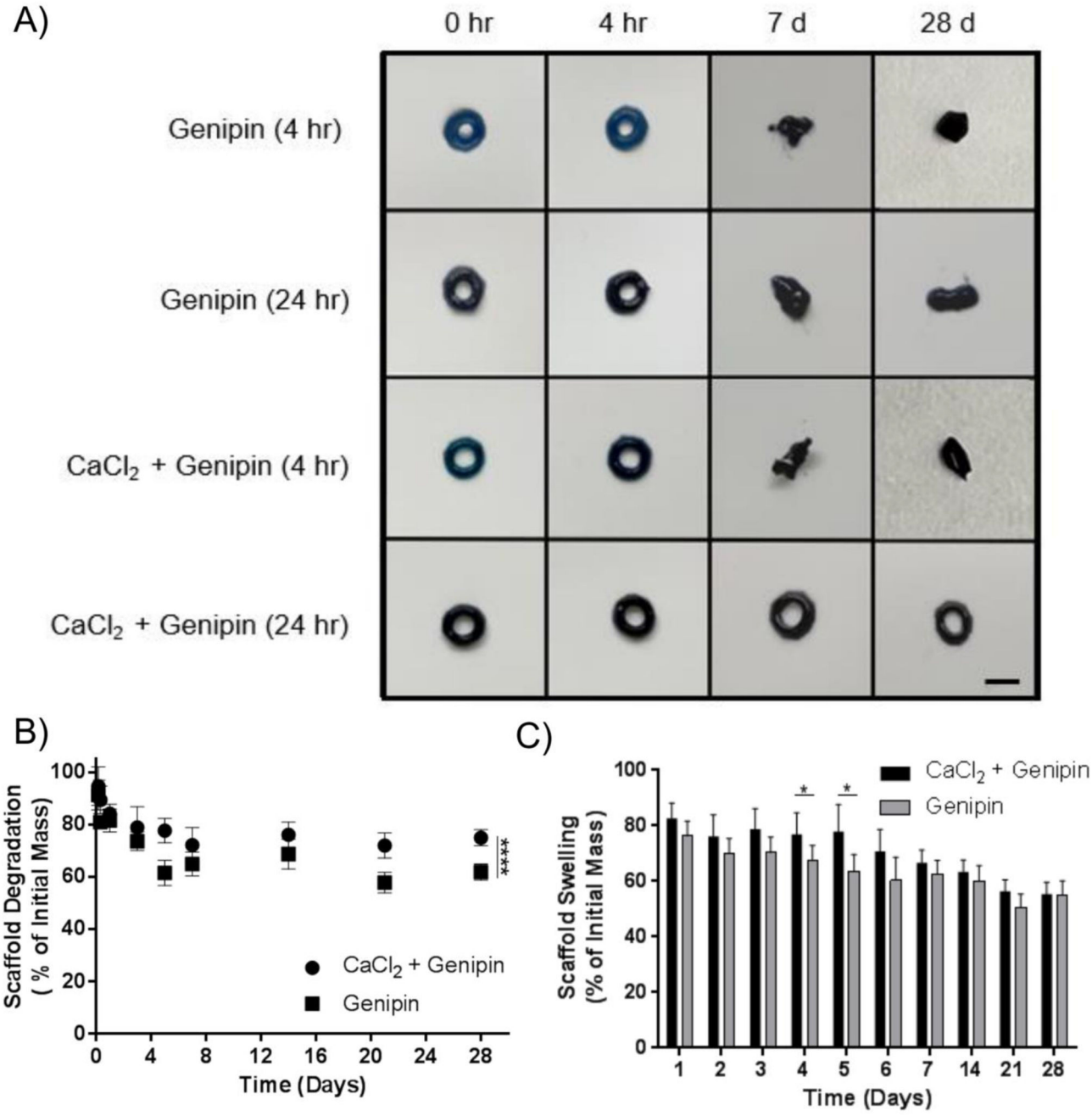

Figure 3.

Scaffold degradation and swelling as a function of crosslinker and crosslinking duration. (A) Representative images of ring-shaped *L. crispatus*-containing scaffolds (outer diameter: 4 mm, inner diameter: 3 mm) printed with 5×10^7 CFU *L. crispatus* per mg scaffold and crosslinked with genipin-only or both $CaCl_2$ and genipin for 4 or 24 hr. Scaffold macrostructure was evaluated after incubation in 5 mL MRS media after 0 and 4 hr, and 7 and 28 d. Scale bar represents 4 mm. Scaffolds printed with $CaCl_2$-only dissolved immediately upon exposure to media (not shown). (B) Scaffold mass loss, attributed to

degradation, and (C) scaffold swelling, both shown as percent of initial mass, for scaffolds dual-crosslinked with $CaCl_2$ and genipin, or genipin-only for 24 hr, were evaluated for 28 d in SVF. Degradation and swelling (mass loss) values are shown as the mean ± standard deviation from five independent ring scaffolds. Statistical significance between experimental groups, as calculated by one-way ANOVA, is represented by *$p \leq 0.05$ and ****$p \leq 0.0001$.

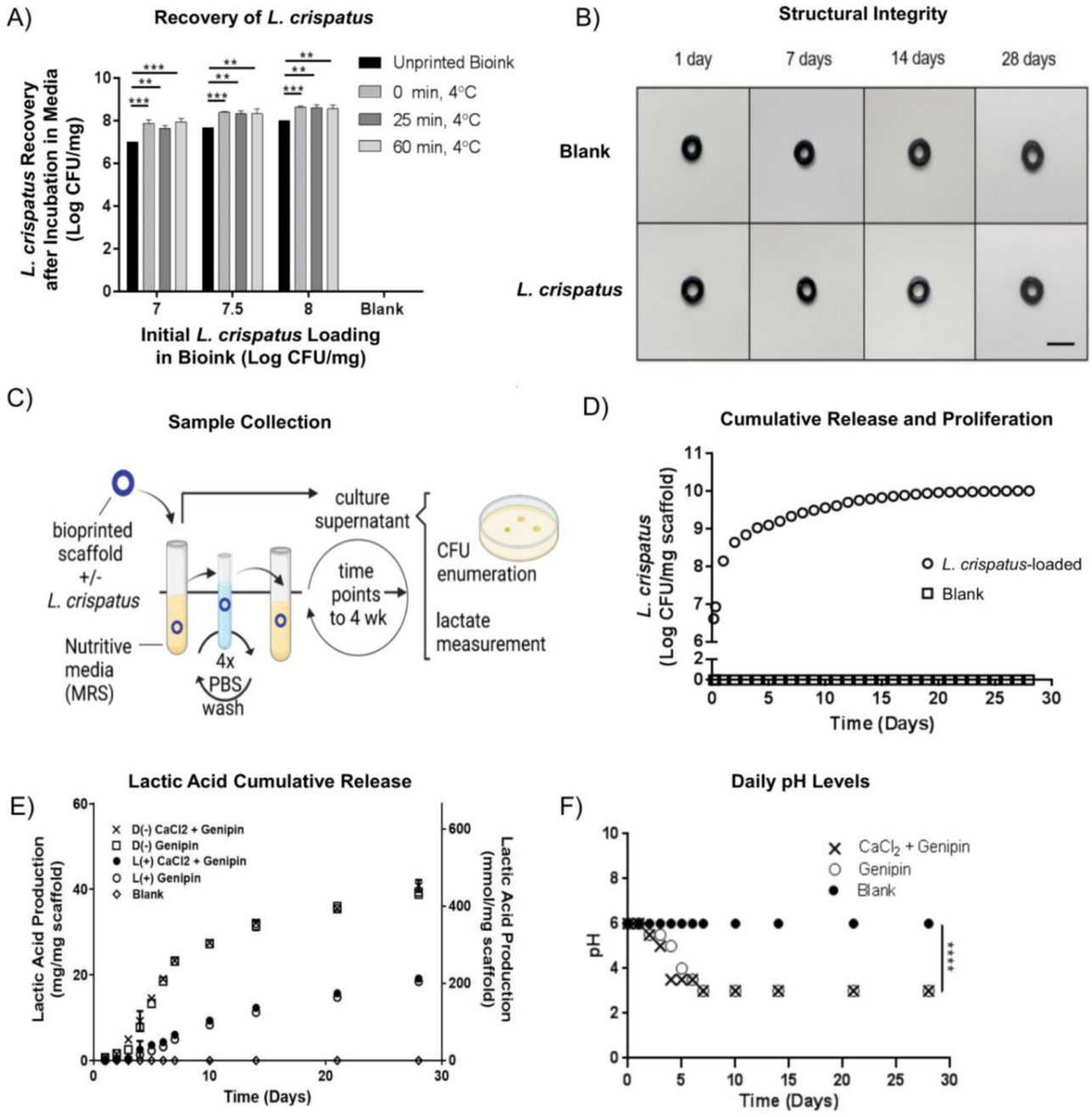

Figure 4.

Evaluation of *L. crispatus* viability, structural integrity, cumulative and daily release/proliferation, and pH modulation from bioprinted scaffolds. (A) Recovery of *L. crispatus* from non-crosslinked 3D printed scaffolds alongside the unprinted bioink containing *L. crispatus*. Samples were incubated in MRS media after different durations at 4°C. (B) Representative images of blank or *L. crispatus*-containing (5×10^7 CFU/mg) ring-shaped scaffolds dual-crosslinked with $CaCl_2$ followed by genipin for 24 hr, and after different immersion durations in SVF (1, 7, 14, 28 d). Scale bar represents 5 mm. (C) Schematic of

incubations of 3D printed devices in MRS media, washing between timepoints, and CFU enumeration. (D) Cumulative release and proliferation of *L. crispatus* in MRS from dual $CaCl_2$ and genipin scaffolds crosslinked for 24 hr. Values are shown as mean ± standard deviation from five independent ring-shaped scaffolds. E) Lactic acid production, in terms of enantiomers, L(+) and D(−) lactic acid, and crosslinking conditions (24 hr), and (F) resulting pH of the scaffold-seeded cultures are shown as the mean ± standard deviation. Error bars are displayed, but are smaller than the symbol size. Statistical significance between experimental groups, as calculated by one-way ANOVA, is represented by **$p \leq 0.01$, ***$p \leq 0.001$ and ****$p \leq 0.0001$.

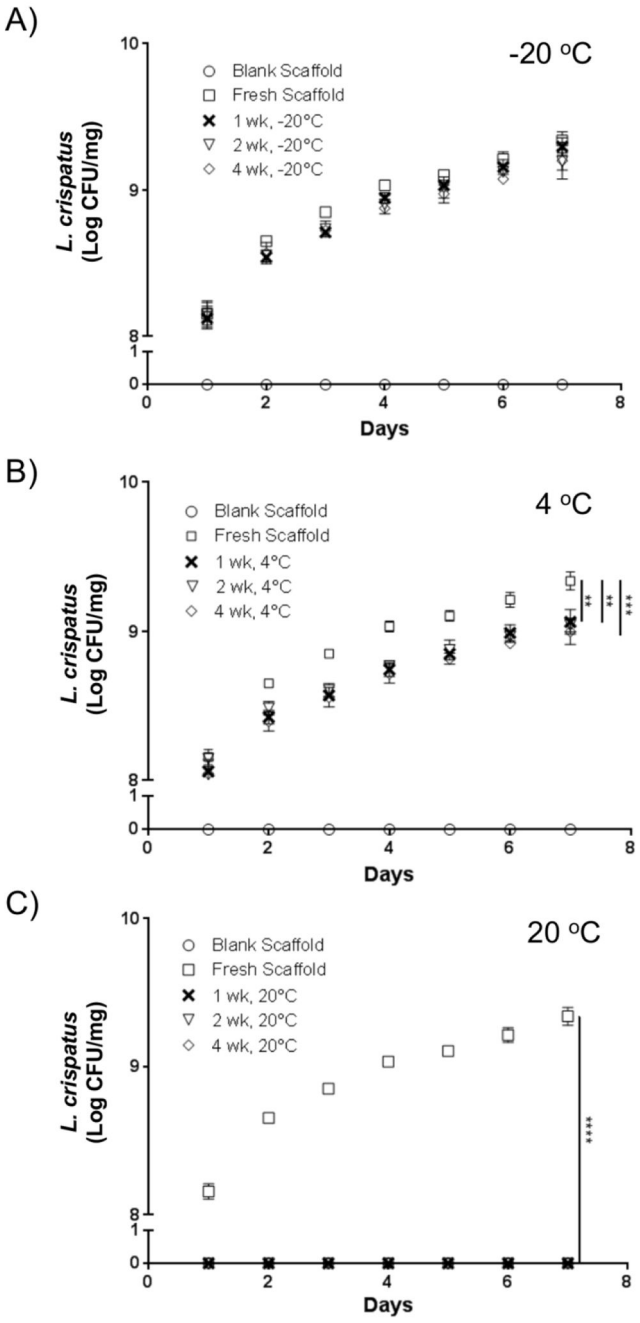

Figure 5.

Stability of dual-crosslinked scaffolds ($CaCl_2$ + genipin, 24hr) after storage. *L.crispatus* viability for 1, 2, and 4 wk in (A) freezer (−20 °C), (B) refrigerator (4 °C), and (C) room temperature (20°C) conditions. Recovery values are shown over 7 d as the mean ± standard deviation of *L. crispatus* from the scaffold-seeded cultures of three independent ring-shaped scaffolds. In some cases, error bars are smaller than the symbol size. Please note overlap in all symbols, with zero viability except for the fresh scaffold in panel C. Statistical

significance between experimental groups, as calculated by one-way ANOVA, is represented by **p≤0.01, ***p≤0.001, and ****p≤0.0001.

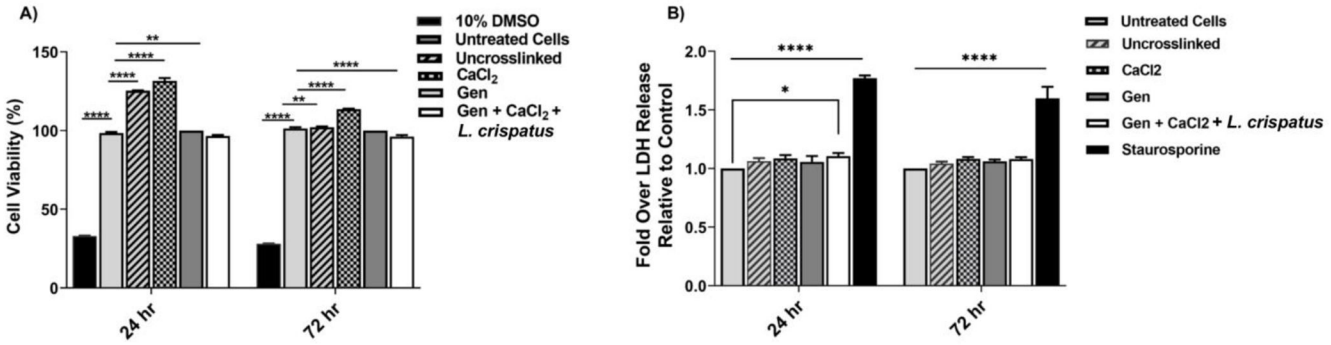

Figure 6.

Cell viability of vaginal keratinocytes (VK2/E6E7 cells) treated with bioprinted scaffolds for 24 or 72 hr. (A) Negligible cytotoxicity was observed in VK2/E6E7 cells administered IVRs that were processed with different crosslinking conditions. (B) No significant release of LDH was observed from VK2/E6E7 cells treated with bioprinted scaffolds for 24 or 72 hr, relative to untreated (control) cells. Cells treated with staurosporine showed significantly elevated LDH levels. Data represent mean±SD (n=5). Statistical significance between experimental groups, as calculated by one-way ANOVA, is represented by *$p \leq 0.05$, **$p \leq 0.01$ and ****$p \leq 0.0001$.

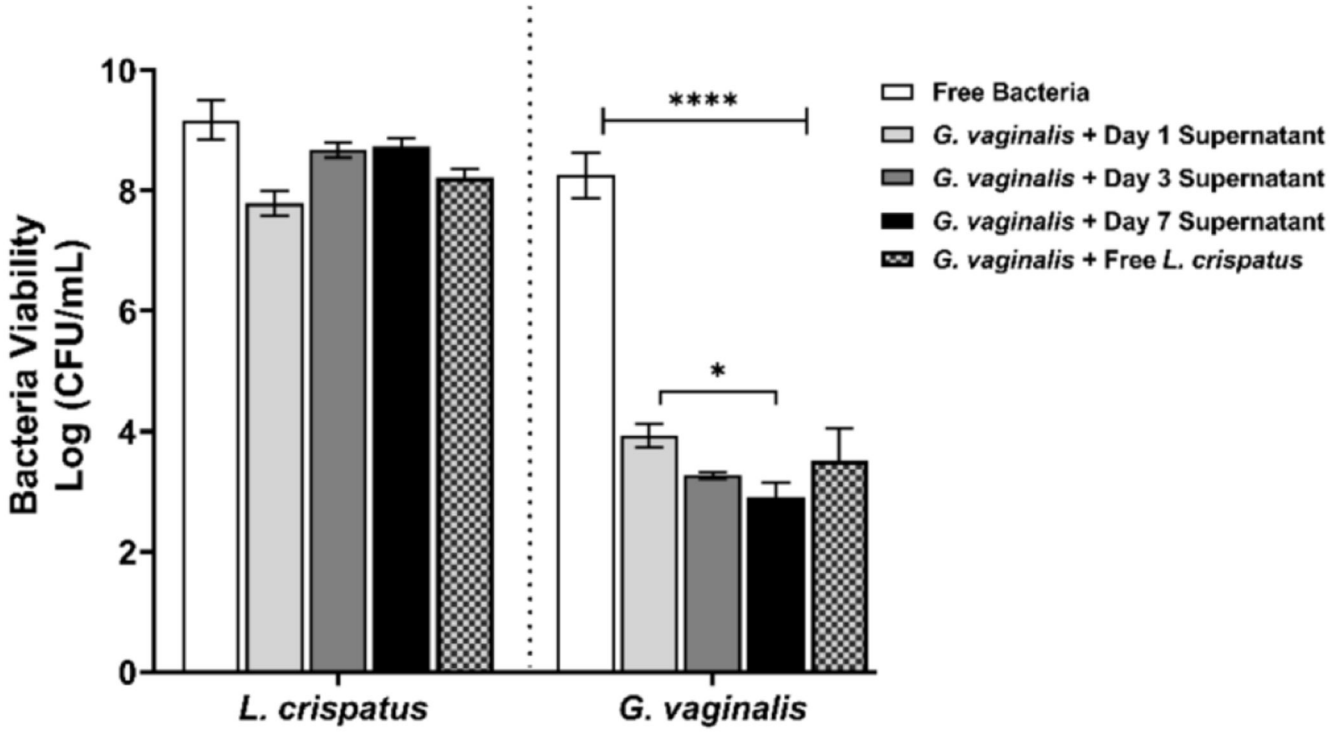

Figure 7.

L. crispatus and G. vaginalis viability when co-cultured with *G. vaginalis* in the presence of VK2 cells exposed to supernatant from *L. crispatus*-loaded bioprinted scaffolds. Data represent mean±SD (n=5). Statistical significance between experimental groups, as calculated by one-way ANOVA, is represented by *$p \leq 0.05$, and ****$p \leq 0.0001$.